ÉNERGIE ET INNOVATION : RECHERCHE / ÉTUDE & SYNTHÈSE

LES CAHIERS DE L'ÉCONOMIE

IFP SCHOOL - IFPEN N° 140 FÉVRIER • 2021

RECHERCHE

TRAJECTORY BASED ROBUST OPTIMIZATION APPLIED TO THE CASE OF ELECTRICITY FACILITIES INVESTMENT WITH SIGNIFICANT PENETRATION OF RENEWABLES

Pierre Cayet
Arash Farnoosh

La collection "Les Cahiers de l'Économie" a pour objectif de présenter les travaux réalisés à IFP Energies nouvelles et IFP School qui traitent d'économie, de finance ou de gestion de la transition énergétique. La forme et le fond peuvent encore être provisoires, notamment pour susciter des échanges de points de vue sur les sujets abordés. Les opinions exprimées dans cette collection appartiennent à leurs auteurs et ne reflètent pas nécessairement le point de vue d'IFP Energies nouvelles ou d'IFP School. Ni ces institutions ni les auteurs n'acceptent une quelconque responsabilité pour les pertes ou dommages éventuellement subis suite à l'utilisation ou à la confiance accordée au contenu de ces publications.

Pour toute information sur le contenu, contacter directement l'auteur.

The collection "Les Cahiers de l'Économie" aims to present work carried out at IFP Energies nouvelles and IFP School dealing with economics, finance or energy transition management . The form and content may still be provisional, in particular to encourage an exchange of views on the subjects covered. The opinions expressed in this collection are those of the authors and do not necessarily reflect the views of IFP Energies nouvelles or IFP School. Neither these institutions nor the authors accept any liability for loss or damage incurred as a result of the use of or reliance on the content of these publications.

For any information on the content, please contact the author directly.

Pour toute information complémentaire
For any additional information

Victor Court
IFP School
Centre Economie et Management de l'Energie
Energy Economics and Management Center
victor.court@ifpen.fr
Tél +33 1 47 52 73 17

Trajectory Based Robust Optimization Applied to the Case of Electricity Facilities Investment with Significant Penetration of Renewables

Pierre CAYETa*, Arash FARNOOSHa

* Corresponding author: *Email address*: pierre.cayet@ifpen.fr ; *postal address:* IFP School, 232 Avenue Napoléon Bonaparte, 92852 Rueil-Malmaison, France

a. IFPEN, IFP School, Center for Energy Economics & Management, 232 Avenue Napoléon Bonaparte, 92852 Rueil-Malmaison, France

Keywords: OR in energy, Uncertainty modelling, Decision analysis, Renewables, Robust optimization

Abstract:

As large scale penetration of renewables into electric systems requires increasing flexibility from dispatchable production units, the electricity mix must be designed in order to address brutal variations of residual demand. Inspired from the philosophy of Distributionally Robust Optimization (DRO), we propose a *trajectory ambiguity set* including residual demand trajectories verifying both support and variability criterion using ambiguous quantile information. We derive level-maximizing, level-minimizing and variability-maximizing residual demand trajectories using two algorithms based on forward-backward path computation. This set of limiting trajectories allows us to make investment decisions robust to extreme levels and brutal variations of residual demand. We provide a numerical experiment using a MILP (Mixed-Integer Linear Programming) investment and unit commitment model in the case of France and discuss the results.

I- Introduction

Modeling time-varying weather events is a pivotal element in investment and operational decisions for electricity production systems, especially when the share of renewables in the production mix is important. Weather dynamics that affect electricity demand and renewable energy sources (RES) availability are characterized by non-normal distributions, autocorrelation and cross-correlations, in addition to cycles following various time scales (seasonal and daily). Net load uncertainties have a direct impact on the level of risks taken by investors when financing new production units (**De Sisternes, 2016 ; Alvarez Lopez & Kumaraswamy, 2010**) and on mechanisms required for adequate remuneration. These uncertain features need to be precisely modeled in optimization models in order to take informed investment and dispatching decisions. However, the distributions of electricity demand and RES availability parameters are often subject to uncertainties. In this paper, we provide a set of tools inspired from distributionally robust optimization in order to derive a set of extreme trajectories of a set of uncertain parameters. The originality of our work lies in a richer definition of robustness, conceived not only as a protection against extreme values of an uncertain parameter but also against its most extreme variations in time.

Traditional approaches to optimization under uncertainty (**Babonneau et al., 2009**) include stochastic optimization (SO) (**Birge & Louveaux, 1997; Kall & Wallace, 1994**), chance-constrained programming (**Charnes & Cooper, 1959; Prékopa, 1970**) and stochastic dynamic programming (**Bellman, 1957; Ross, 1983; Bertsekas, 1995**). These models assume the perfect knowledge of a well-defined probability model of an uncertain parameter. In the deterministic formulation of stochastic optimization, each value of the parameter is associated with a scenario with a positive probability of occurrence. This results in high complexity and makes the computation of the solution quickly intractable for large models. Moreover, solutions are highly sensitive to errors in the estimation of the distribution of the uncertain parameter. First proposed by **Soyster (1973)**, robust optimization (RO) adopts a non-probabilistic formulation of uncertainty and only requires knowledge of the support of the distribution of uncertainties. The idea of robust optimization is to determine solutions that remain satisfactory for all realizations of the uncertain parameters, by hedging against the worst-case. In order to avoid over-conservative solutions, recent work focused on the development of more elaborate uncertainty sets of parameters (**Ben-Tal & Nemirovski, 2000; Bertsimas & Sim, 2004)**, introducing uncertainty budgets, asymmetries in the distribution of uncertainties (**Chen et al, 2007**), correlated uncertainties (**Yuan et al., 2016; Jalilvand-Nejad et al., 2016; Ning & You, 2018**) and dynamic uncertainty sets (**Lorca & Sun, 2014**).

Distributionally robust optimization (DRO) is an emerging approach combining insights from SO and RO by searching for a solution that optimizes the worst-case expected performance on a set of distributions of the uncertain parameters, referred to as the ambiguity set. Contrary to SO, DRO does not require knowledge of the entire distribution of the uncertain parameters, but only information about its moments, which makes it increasingly popular (**Shapiro & Nemirovski, 2005; Goh & Sim, 2010; Wiesemann et al., 2014; Yue & You, 2016**). The ambiguity set can be moment-based or metric-based: in

the first case, it includes all distributions of uncertain parameters with common support set and moment statistics, which are estimated from available empirical data, while the latter includes all probability distributions within a certain distance from the a nominal distribution for a given distance metric. Recent developments on ambiguity sets include higher order moments and "entropic dominance" as a new characterization of stochastic independence of uncertainty (**Chen et al., 2019)**. The use of DRO models is becoming increasingly popular for modeling power dispatch, power flows and production planning in the electricity sector (**Chen et al., 2016; Ma et al., 2020; Shang & You, 2018; Dong et al, 2019**).

In order to properly model decisions involving stochastic processes, DRO coupled with Markov Decision Processes with uncertain transition probabilities and reward parameters provides a popular approach. **Xu & Mannor (2012)** describe uncertainty using a sequence of nested ambiguity sets and propose a decision criterion based on "distributional robustness". **Yu & Xu (2015)** propose a general class of state-wise ambiguity sets and derive tractable distributionally robust MDPs under mild assumptions. Under similar uncertain conditions, **Nakao et al. (2019)** build an ambiguity set of the joint distribution using bounded moments and propose state-wise piecewise linear convex approximations of Bellman value functions with a heuristic iteration method allowing to derive its lower and upper bounds.

Instead of modeling uncertain states with their associated transition probabilities within a process, we define longitudinal clusters of each component of multidimensional random process and construct a *trajectory ambiguity set* for each cluster. This set includes all probability distributions of a given stochastic process with their quantiles included in a ball centered on the empirical quantile value. Similarly, the distribution of the variations between two consecutive quantile values in the stochastic process has each quantile centered around each quantile value of the empirical distribution of variations. The radius of these balls are defined as functions of both the number of quantiles considered and the number of observations in the training dataset. This framework allows us to refine the usual definition of robustness. Robustness is usually implicitly considered as hedging against the highest or lowest value an uncertain vector of parameters can take. Yet, in the case of electric systems with high renewables penetration, system flexibility is increasingly required and valued. Thus, it seems appropriate to define a production mix that is also robust to the most extreme variations of the uncertain parameters, namely electric load, solar and wind capacity factors. Using a combination of backward and forward iterative computations to calculate the most volatile path between consecutive values of the uncertain parameter, we propose two polynomial time algorithms allowing to determine the variability-maximizing and level-maximizing trajectories of the uncertain parameters' quantiles. A set of worst-case trajectories can then be defined for each possible distribution included in the *trajectory ambiguity set*. Finally, we propose a numerical experiment, using our original framework for electricity mix optimal investment decisions under residual demand uncertainty in the case of one of the most industrial French regions. We provide a discussion of the results and hints for further research and improvement of the simplified framework proposed in this paper.

Section II details our clustering and DRO-inspired methodology in a quantile information framework, providing theoretical properties for our *trajectory ambiguity set* and two original algorithms for computing worst-case trajectories. Section III proposes a numerical simulation using a cost minimizing optimization model for the electricity mix of the French region Auvergne Rhône-Alpes. We compare solutions obtained when using only level robustness and both level and variability robustness, before concluding in Section IV.

II- Methodology

Our method first consists in clustering individual cyclical components of residual demand in order to identify patterns in their trajectories. Then, we propose an extended version of the ambiguity set proposed by **Delage & Ye (2010)**, called *trajectory ambiguity set*, in order to include uncertainty in the quantity of variations of the uncertain parameter. We provide its theoretical properties with proofs in addition to an algorithmic method for estimating the most-adverse trajectories.

II.1. Clustering methodology

II.1.1. Definitions

We define the multidimensional random process of dimension $|I| \times |T|$, $\{\boldsymbol{\xi_t}\}_{t\in T} = \left(\{\xi_{it}\}_{\substack{t\in T \\ i\in I}}\right)$. We assume $\{\boldsymbol{\xi_t}\}_{t\in T}$ takes discrete values. Furthermore, we assume individual components of $\{\boldsymbol{\xi_t}\}_{t\in T}$ have different scales and are not commensurable. The first step of our method consists in determining statistical patterns in the trajectories of each component $i \in I$ of our random process. $\{\boldsymbol{\xi_t}\}_{t\in T}$ can be decomposed as the stacking of I one dimensional random vectors $\{\xi_{it}\}_{t\in T}$, with $i \in I$. We assume that $\forall i \in I$, $\{\xi_{it}\}_{t\in T}$ is a weakly cyclically stationary stochastic process of period P, such that $\forall t' \in T$, $\mathbb{E}(\xi_{it'}) = \mathbb{E}(\xi_{it'+nP})$ and $\mathbb{V}(\xi_{it'}) = \mathbb{V}(\xi_{it'+nP})$, for $n \in \mathbb{N}^*$, where $\mathbb{N}^*$ is the set of strictly positive integers. Finally, we define the support of $\{\boldsymbol{\xi_t}\}_{t\in T}$ as $\Xi = \prod_{t\in T} \Xi_t = \prod_{t\in T}\prod_{i\in I} \Xi_{it}$, where $\xi_{it} \in \Xi_{it}, \forall t \in T, \forall i \in I$.

$\{\boldsymbol{\xi_t}\}_{t\in T}$ can thus be decomposed into the reunion of several cyclical stochastic processes of period P such that $\{\boldsymbol{\xi_t}\}_{t\in T} = \left(\{\boldsymbol{\xi_\tau}\}_{\tau\in[0,P]}, \{\boldsymbol{\xi_{\tau+P}}\}_{\tau\in[0,P]}, \cdots, \{\boldsymbol{\xi_{\tau+(N-1)P}}\}_{\tau\in[0,P]}\right)$, where $N = T \times P^{-1}$. In a similar fashion, $\{\boldsymbol{\xi_{it}}\}_{t\in T}$ can be decomposed into a reunion of stochastic processes such that $\{\boldsymbol{\xi_{it}}\}_{t\in T} = \left(\{\boldsymbol{\xi_{i\tau}}\}_{\tau\in[0,P]}, \{\boldsymbol{\xi_{i\tau+P}}\}_{\tau\in[0,P]}, \cdots, \{\boldsymbol{\xi_{i\tau+(N-1)P}}\}_{\tau\in[0,P]}\right)$.

The clustering step consists in identifying in the data, for each $\{\boldsymbol{\xi_{it}}\}_{t\in T}, i \in I$, different clusters of trajectories of period P, where a cluster includes all trajectories which share similar statistical properties. A number of relevant statistical measures can be used to identify patterns in individual longitudinal

trajectories **(Leffrondree et al.,2004; Sylvestre et al, 2006)**, including range, mean over time, standard deviation, coefficient of variation, maximum and standard deviation of the first differences. A subset of these measures is selected using factor analysis and then used for clustering analysis. This first clustering step is performed through using a statistical program (modeled in R and using the package *traj.*) For $i \in I$, the corresponding set of clusters is noted S_i with elements $s_i^{j_i} \in S_i$, where $j_i \in [1, |S_i|]$. Each $s_i^{j_i}$ thus corresponds to a subset of trajectories with similar statistical characteristics.

Once clusters of trajectories have been determined for each $\{\boldsymbol{\xi_{it}}\}_{t\in T}$, we further identify a set of "meta-clusters" noted $\sigma \in \Sigma$, in order to identify associative patterns between individual clusters of trajectories. "Meta-clusters" correspond to the set of exogenous conditions which generate a combination of clusters for each component of $\{\boldsymbol{\xi_t}\}_{t\in T}$. By construction, we assign a single meta cluster to each period of length P, where σ_n is associated with the trajectory $\{\boldsymbol{\xi_{\tau+nP}}\}_{\tau\in[0,P]}, \forall n \in [0, N-1]$. In the case of electricity generation, "meta-clusters" can be defined as the set of exogenous meteorological conditions which jointly determine electricity demand trajectories, PV and wind capacity factor trajectories.

For each period of length P, we define the joint state of trajectories as $s_n = (s_1, \dots, s_I) \in \prod_{i=1}^{I} S_i$. Then, for a given combination s_n, if there exists no $\sigma_n \in \Sigma$ such that $\left\{\sigma_n \in \Sigma, n \in [0, N] \mid s_n = \left(s_i^{j_i}\right)_{i\in I}\right\} \neq \emptyset$, we say that s_n is impossible. "Meta-clusters" are computed using the k-means method and their optimal number is determined using the "elbow" method. Note that in the case of residual demand, which is a linear combination of electricity demand and RES production, each element or component had follows a daily cycle with the same period $P = 24$.

II.1.2. Computation of the worst-case joint state of nature

Once clusters are identified for each random vector $\{\xi_{it}\}_{t\in T}$, we determine which trajectory type $s_i^{j_i} \in S_i$ is likelier to produce trajectories taking the highest values within the multidimensional set $\prod_{n=1}^{N-1}\prod_{\tau=1}^{P} \Xi_{i\tau+nP}$. Formally, we note the state in which $\{\boldsymbol{\xi}_{i\tau+nP}\}_{\tau\in[0,P]}$ is more likely to take its highest values (resp. its lowest values) as s_i^+ (resp. s_i^-). As we are also interested in the most volatile types of trajectories, we may further restrict our attention to trajectory types that generate distributions of values with variance superior to a given threshold. Computing s_i^+ is equivalent to measuring which subset $s_i^{j_i} \in S_i$ is second-order stochastically dominated by all other subsets $s_i^{-j_i} \in S_i \setminus \{s_i^{j_i}\}$.

First, we define the matrix $\boldsymbol{\Lambda_i} \in \mathbb{R}^{|S_i|} \times \mathbb{R}^{|S_i|}$, with elements λ_{jk}^i defined such that :

$$\lambda_{jk}^i = \int_0^P \int_0^1 (\inf\{\xi_{i\tau+nP} | F_i(\xi_{i\tau+nP} | s_i = j) \geq q, 0 \leq n \leq N\} - \inf\{\xi_{i\tau+nP} | F_i(\xi_{i\tau+nP} | s_i = k) \geq q, 0 \leq n \leq N\}) dq d\tau \quad (\mathbf{1})$$

where $(j,k) \in [1,|S_i|]^2$ and $F_i(\xi_{it})$ corresponds to the cumulative distribution function of ξ_{it}. We further define the binary matrix $\widetilde{\boldsymbol{\Lambda}}_{\boldsymbol{i}}$ associated to $\boldsymbol{\Lambda}_{\boldsymbol{i}}$, with elements defined ${\lambda^i_{jk}}^+$ such that :

$$ {\lambda^i_{jk}}^+ = \begin{cases} 1 & \text{if} \quad \lambda^i_{jk} > 0 \\ 0 & \text{else} \end{cases} \tag{2} $$

Using this definition of $\widetilde{\boldsymbol{\Lambda}}_{\boldsymbol{i}}$, s_i^+ and s_i^- can respectively be computed as follows:

$$ s_i^+ = \left\{ j \in S_i | \forall j' \in S_i, \sum_k {\lambda^i_{j'k}}^+ \leq \sum_k {\lambda^i_{jk}}^+ \right\} = \arg\max_j \left(\sum_k {\lambda^i_{jk}}^+ \right) \tag{3} $$

$$ s_i^- = \left\{ j \in S_i | \forall j' \in S_i, \sum_k {\lambda^i_{j'k}}^+ \geq \sum_k {\lambda^i_{jk}}^+ \right\} = \arg\min_j \left(\sum_k {\lambda^i_{jk}}^+ \right) \tag{4} $$

The definition of the worst-case joint state of nature noted $s^* \in \prod_{i=1}^I S_i$ is conditional on the type of variables included in the multidimensional random process $\{\boldsymbol{\xi_t}\}_{t\in T}$ and the users' objectives. In the context of electricity generation mix optimization under residual demand uncertainty, the worst-case trajectories corresponds to the cases where residual demand takes its maximal or its minimum values successively. If we assume $\{\boldsymbol{\xi_{1t}}\}_{t\in T}$ corresponds to electricity demand trajectory and $\{\boldsymbol{\xi_{it}}\}_{t\in T}$ corresponds to capacity factor trajectory for renewable generation technology $i, i > 1$, then the worst-case joint states of nature are defined as $s^{*+} = (s_1^+, s_2^-, \dots, s_I^-)$ and $s^{*-} = (s_1^-, s_2^+, \dots, s_I^+)$. Yet, although $\left(s^{*+}, s^{*-}\right)$ are theoretically possible, they may be empirically impossible, i.e. there may exist no "meta-cluster" such that those combinations are generated. Thus, the worst-case joint states of nature that are feasible, defined as $\hat{s}^+$ and $\hat{s}^-$, are respectively the solutions to the following optimization problems:

$$ \hat{s}^+ = \underset{(s_1,\dots,s_I)}{\arg\max} \left(\sum_k \widetilde{\lambda^1_{s_1 k}} + \sum_{i>1} \left(|S_i| - \widetilde{\lambda^i_{s_i k}} \right) \right) $$

$$ s.t. \exists \sigma_n \in \Sigma, \left\{ \sigma_n \in \Sigma, n \in [0,N] \mid s^o \in \prod_{i=1}^I S_i \right\} \neq \emptyset \tag{5a} $$

$$ \hat{s}^- = \underset{(s_1,\dots,s_I)}{\arg\min} \left(\sum_k \widetilde{\lambda^1_{s_1 k}} + \sum_{i>1} \left(|S_i| - \widetilde{\lambda^i_{s_i k}} \right) \right) $$

$$ s.t. \exists \sigma_n \in \Sigma, \left\{ \sigma_n \in \Sigma, n \in [0,N] \mid s^o \in \prod_{i=1}^I S_i \right\} \neq \emptyset \tag{5b} $$

It is important to note that the clustering step is only required for non-commensurable individual stochastic processes. In the case of residual demand, electricity load is typically measured in MWh while

wind and solar capacity factors have no unit. It is thus not possible to aggregate them. If installed capacities in wind and solar units are known *a priori*, it is possible to directly compute the renewable production, which in turns allows us to aggregate components of $\{\boldsymbol{\xi_t}\}_{t\in T}$ into a one dimensional stochastic process corresponding to residual demand.

II.2. Trajectory-based DRO using quantile information

Robust optimization consists in finding a solution that remains feasible in the case where an uncertain parameter takes its worst possible value, yet it may result in overly conservative solutions. On the other hand, DRO consists in finding a solution that maximizes the expected performance (or minimizes the expected cost) under the most adverse distribution of the uncertain parameter. However, the expected performance might not only be a function of ξ_t, but also of $\Delta\xi_t = \xi_t - \xi_{t-1}$. In the case of electricity mix optimization, starting and ramping costs, in addition to technical limitations to the variation of production (minimum production level, minimum-up and down time, ramping limits) may significantly affect the optimal solution. A suboptimal mix in terms of flexibility may result in load shedding or overproduction if dispatchable production units cannot rapidly adjust to residual demand fluctuations. The worst-case distribution of parameters can thus be defined as the distribution of residual demand components that maximizes or minimizes the values taken by residual demand and maximizes the volatility of residual demand trajectories. We define the ambiguity set associated with the multidimensional random process $\{\boldsymbol{\xi_t}\}_{t\in T}$ as $\mathbb{B}$. Let $\boldsymbol{x} \in \mathcal{X} \subseteq (\mathbb{R}^+)^T$ be the decision vector and $h(\boldsymbol{x}, \boldsymbol{\xi}, \boldsymbol{\Delta\xi})\colon \mathcal{X} \times \Xi \longmapsto \mathbb{R}$ be a random cost function (**Rahimian & Mehrotra, 2019)**, increasing both in $\boldsymbol{\xi}$ and $\boldsymbol{\Delta\xi}$. Given this formulation, the robust optimization problem has the following form:

$$\inf_{x\in\mathcal{X}} \left\{ \sup_{\boldsymbol{\xi}\in\mathbb{B}} \{h(\boldsymbol{x}, \boldsymbol{\xi}, \boldsymbol{\Delta\xi})\} \right\} \quad (\mathbf{6})$$

Assuming separability of the cost function and $(\boldsymbol{\xi}, \boldsymbol{\Delta\xi}) \in \mathbb{B}^2$, the robust optimization problem can be reformulated as

$$\inf_{x\in\mathcal{X}} \left\{ \sup_{\boldsymbol{\xi}\in\mathbb{B}} \{h(\boldsymbol{x}, \boldsymbol{\xi})\} + \sup_{\boldsymbol{\xi}\in\mathbb{B}} \{h(\boldsymbol{x}, \boldsymbol{\Delta\xi})\} \right\} \quad (\mathbf{7})$$

II.2.1. Definitions and main properties

Let us start with a general presentation of our approach and drop subscript i without loss of generality. We define the *trajectory ambiguity set* associated with the distribution of $\{\boldsymbol{\xi_t}\}_{t\in T}$ as follows:

$$\mathbb{B} = \left\{ \xi_t \in \Xi_t, t \in T \middle| \begin{array}{ll} \mathbb{P}(\xi_t \in \Xi_t) = 1 & (\mathbf{8}) \\ \left| F_t^{\leftarrow}(q) - \xi_t^{(q)} \right| \leq \beta_q & (\mathbf{9}) \\ \left| F_t^{\leftarrow}(\dot{q}, r) - \left(\dot{\xi}_t \middle|_{\xi_{t-1}=\xi_{t-1}^{(q)}} \right)^{(r)} \right| \leq \alpha_{qr} & (\mathbf{10}) \end{array} \right\}$$

We assume that the true support of the unknown parameter, denoted by Ξ_t, is unknown. The originality of our work is summarized in constraints **(9)** and **(10)**. For $q \in \mathcal{Q} \subseteq \mathbb{N}^*$ and $|\mathcal{Q}|$ the cardinal of $\mathcal{Q}$, we note $F_t^{\leftarrow}(q) = \inf_{\xi_t \in \Xi_t} \left\{ \xi_t : F(\xi_t) \geq \frac{q}{|\mathcal{Q}|} \right\}$ the theoretical q-th quantile of ξ_t, while $\xi_t^{(q)}$ corresponds to its empirical q-th quantile. In a similar fashion, for $r \in \mathcal{R} \subseteq \mathbb{N}^*$, we define $F_t^{\leftarrow}(\dot{q}, r) = \inf_{\dot{\xi}_t \in \mathbb{R}} \left\{ \dot{\xi}_t : F\left(\dot{\xi}_t | \xi_{t-1} = \xi_{t-1}^{(q)} \right) \geq \frac{r}{|\mathcal{R}|} \right\}$ as the r-th quantile in the conditional distribution of $\dot{\xi}_t | \xi_{t-1}^{(q)}$, while $\left(\dot{\xi}_t \middle|_{\xi_{t-1}=\xi_{t-1}^{(q)}} \right)^{(r)}$ corresponds to the r-th quantile in the empirical conditional distribution of $\dot{\xi}_t | \xi_{t-1}^{(q)}$. Finally, $\forall q \in \mathcal{Q}, \forall r \in \mathcal{R}, \beta_q, \alpha_{qr} \geq 0$.

We note the vector of quantile values $\boldsymbol{\epsilon}_t = \left(\xi_t^{(0)}{}_t, \xi_t^{(1)}, \dots, \xi_t^{(k)}, \dots, \xi_t^{(|\mathcal{Q}|)}, \xi_t^{(|\mathcal{Q}|+1)} \right)$, where the minimum and maximum empirical values $\xi_t^{(0)}$ and $\xi_t^{(|\mathcal{Q}|+1)}$ are such that $\xi_t^{(0)} \geq \inf_{\xi_t} \Xi_t$ and $\xi_t^{(|\mathcal{Q}|+1)} \leq \sup_{\xi_t} \Xi_t$. The ambiguity pertains to the values of the parameters β_q and α_{qr}: higher values indicate the true values of quantiles of the distribution of $\xi_t^{(q)}$ and $\left(\dot{\xi}_t \middle|_{\xi_{t-1}=\xi_{t-1}^{(q)}} \right)^{(r)}$ may lie further away from the empirically measured values. Each quantile is constrained to lie within a ball of radius β_q or α_{qr} centered on $\xi_t^{(q)}$ and $\left(\dot{\xi}_t \middle|_{\xi_{t-1}=\xi_{t-1}^{(q)}} \right)^{(r)}$ respectively. Let us define the empirical distribution of ξ_t such that:

$$\mathbb{P}_N(\xi_t = \xi) = \frac{1}{N} \sum_{n=1}^{N} \delta_{\xi_{nt}}(\xi) \qquad (\mathbf{11})$$

Where $\delta_{\xi_{nt}}(\xi)$ denotes the Dirac measure at point ξ_{nt}, $n \leq N$, and N is the number of observations in the training sample (**Kuhn et al., 2019**). For any $q \in \mathcal{Q}$, we can thus define $\xi_t^{(q)}$ as

$$\xi_t^{(q)} = \inf_{\xi_t \in \mathbb{B}} \left\{ \xi_t : \sum_{\xi_{t'} \leq \xi_t} \mathbb{P}_N(\xi_t = \xi_t') \geq \frac{q}{|\mathcal{Q}|} \right\} = \inf_{\xi_t \in \mathbb{B}} \left\{ \xi_t : \sum_{\xi_{t'} \leq \xi_t} \left(\frac{1}{N} \sum_{n=1}^{N} \delta_{\xi_{nt}}(\xi_t') \right) \geq \frac{q}{|\mathcal{Q}|} \right\} \qquad (\mathbf{12})$$

Assume $\mathbb{P}_N(\xi_t = \xi)$ is an unbiased estimate of the true probability of $\xi \in \Xi_t$. Then, as the variance of the estimator $\mathbb{P}_N(\xi_t = \xi)$ decreases with N, the variance of $\xi_t^{(q)}$ decreases also with N and we can show that, for $\varepsilon > 0$:

$$\mathbb{P}\left(\left| \xi_t^{(q)} - F_t^{\leftarrow}(q) \right| > \varepsilon \right) \leq \mathbb{P}\left(\left| \xi_t^{(q)} - \mathbb{E}\left(\xi_t^{(q)} \right) \right| > \frac{\varepsilon}{2} \right) \leq \frac{4\mathbb{V}\left(\xi_t^{(q)} \right)}{\varepsilon^2} \to 0,$$

$N \to +\infty$, using the Chebyshev's inequality. The same holds for the distribution of variations of the uncertain parameter. Thus, we can define β_q, α_{qr} as decreasing functions of N and increasing functions of $|\mathcal{Q}|$ and $|\mathcal{R}|$ respectively. By noting $\mathcal{Q}_N = \frac{|\mathcal{Q}|}{N}$, $\mathcal{R}_\mathcal{Q} = \frac{|\mathcal{R}||\mathcal{Q}|}{N}$, and by defining $m_q = \left|q - \left\lfloor \frac{|\mathcal{Q}|}{2} \right\rfloor\right|$, $m_r = \left|r - \left\lfloor \frac{|\mathcal{R}|}{2} \right\rfloor\right|$ the distance to the median quantile, we can define the functions β_q,α_{qr} as

$$\beta_q = \beta\left(m_q, \mathcal{Q}_N\right), \frac{\partial \beta(m_q, \mathcal{Q}_N)}{\partial m_q} > 0, \frac{\partial \beta(m_q, \mathcal{Q}_N)}{\partial \mathcal{Q}_N} > 0$$

$$\alpha_{qr} = \alpha\left(m_r, \mathcal{Q}_N, \mathcal{R}_\mathcal{Q}\right), \frac{\partial \alpha(m_r, \mathcal{Q}_N, \mathcal{R}_\mathcal{Q})}{\partial \mathcal{R}_\mathcal{Q}} > 0, \frac{\partial \alpha(m_r, \mathcal{Q}_N, \mathcal{R}_\mathcal{Q})}{\partial m_r} > 0,$$

where the positive signs when deriving with respect to m_q and m_r translate the fact that the ambiguity of measure is expected to increase for extreme events. As the number of observations may be low for such events, higher values of β_q and α_{qr} ensure the ambiguity set includes extreme tail values of the uncertain parameter that have not yet been observed in the training dataset.

It is possible to relate our *trajectory ambiguity set* to a moment-based ambiguity set (**Delage & Ye, 2010**) by approximating its moments. For instance, using information on the vector $\boldsymbol{\beta} = \left(\beta_q\right)_{q \in \mathcal{Q}}$, it is possible to define a set $\mathcal{U}_t$ such that:

$$\mathcal{U}_t = \left\{ \sum_{q \in \mathcal{Q}} \omega_q \left(\xi_t^{(q)} + \widehat{\beta_q}\right) | \widehat{\boldsymbol{\beta}} = \left(\left(\widehat{\beta_q}\right)_{q \in \mathcal{Q}}\right), -\beta_q \leq \widehat{\beta_q} \leq \beta_q \right\} \quad (\mathbf{13})$$

With $\omega_q = \frac{1}{|\mathcal{Q}|+1}$. We bound the expected value of ξ_t, $\mathbb{E}(\xi_t)$, by successively pushing all the mass into the inferior bound and the upper bound of each of the $|\mathcal{Q}| + 1$ intervals:

$$\mu_t^- = \inf_{\left(\widehat{\beta_q}\right)_{q \in \mathcal{Q}}} \mathcal{U}_t = \sum_{q \in \mathcal{Q} \setminus \{|\mathcal{Q}|+1\}} \omega_q \left(\xi_t^{(q)} - \beta_q\right) \quad (\mathbf{14})$$

$$\mu_t^+ = \sup_{\left(\widehat{\beta_q}\right)_{q \in \mathcal{Q}}} \mathcal{U}_t = \sum_{q \in \mathcal{Q} \setminus \{0\}} \omega_q \left(\xi_t^{(q)} + \beta_q\right) \quad (\mathbf{15})$$

As $\mu_t^- \leq \mathbb{E}(\xi_t) \leq \mu_t^+$ and $(\mu_t^+, \mu_t^-) \subseteq \mathcal{U}_t$, then $\mathbb{E}(\xi_t) \in \mathcal{U}_t$. It is then straightforward to verify that $\mathcal{U}_t \to \{\mathbb{E}(\xi_t)\}$ as $N \to +\infty$ and $|\mathcal{Q}| \to |\Xi_t|$.

Finally, due to the ambiguity of the measure of quantile values, the probability that the uncertain parameter lies within a given set is itself a function of this ambiguity, which is captured by the vector $\boldsymbol{\beta} = \left(\left(\beta_q\right)_{q \in \mathcal{Q}}\right)$. In order to formalize this intuition, let us define the subset $\Xi_t(q, q') = \left[\xi_t^{(q)}, \xi_t^{(q')}\right] \subseteq$

Ξ_t, $\forall (q, q') \in \mathcal{Q}, \forall t \in T$. Then, for all subset $\Xi_t{}' \subseteq \Xi_t$, it is possible to define $\mathcal{Q}$ and identify a couple $(q, q') \in \mathcal{Q}$ such that:

$$\mathbb{P}(\xi_t \in \Xi_t{}') \leq \mathbb{P}\left(\xi_t \in \Xi_t(q,q') | \inf_q \Xi_t(q,q') \geq \inf \Xi_t, \sup_{q'} \Xi_t(q,q') \leq \sup \Xi_t\right) \quad (16)$$

Then:

$$\mathbb{P}(\xi_t \in \Xi_t{}') \leq \mathbb{P}\big(\xi_t \in \Xi_t(q,q')\big)$$

$$= \mathbb{P}\left(\xi_t \in \Xi_t | \xi_t \leq \xi_t^{(q')}\right) - \mathbb{P}\left(\xi_t \in \Xi_t | \xi_t \leq \xi_t^{(q)}\right)$$

$$\leq \mathbb{P}\left(\xi_t \in \Xi_t | \xi_t \leq \xi_t^{(q')} + \beta_{q'}\right) - \mathbb{P}\left(\xi_t \in \Xi_t | \xi_t \leq \xi_t^{(q)} - \beta_q\right)$$

Similarly, $\mathbb{P}\big(\xi_t \in \Xi_t(q,q')\big) \geq \mathbb{P}\left(\xi_t \in \Xi_t | \xi_t \leq \xi_t^{(q')} - \beta_{q'}\right) - \mathbb{P}\left(\xi_t \in \Xi_t | \xi_t \leq \xi_t^{(q)} + \beta_q\right)$. Then, by noting $\psi^+(\xi_t, \beta_q) = \mathbb{P}\left(\xi_t \in \Xi_t | \xi_t^{(q)} < \xi_t \leq \xi_t^{(q)} + \beta_q\right)$ and $\psi^-(\xi_t, \beta_q) = \mathbb{P}\left(\xi_t \in \Xi_t | \xi_t^{(q)} - \beta_q \leq \xi_t < \xi_t^{(q)}\right)$, we have:

$$\frac{q'-q}{|\mathcal{Q}|+1} - \left(\psi^+(\xi_t, \beta_q) + \psi^-(\xi_t, \beta_{q'})\right) \leq \mathbb{P}\big(\xi_t \in \Xi_t(q,q')\big) \leq \frac{q'-q}{|\mathcal{Q}|+1} + \left(\psi^+(\xi_t, \beta_{q'}) + \psi^-(\xi_t, \beta_q)\right)$$

Using a similar reasoning in order to derive a lower bound for $\mathbb{P}(\xi_t \in \Xi_t{}')$, we can provide it with the following bounds, with $(p, p') \in \mathcal{Q}$:

$$\frac{p'-p}{|\mathcal{Q}|+1} - \left(\psi^+(\xi_t, \beta_p) + \psi^-(\xi_t, \beta_{p'})\right) \leq \mathbb{P}(\xi_t \in \Xi_t{}') \leq \frac{q'-q}{|\mathcal{Q}|+1} + \left(\psi^+(\xi_t, \beta_{q'}) + \psi^-(\xi_t, \beta_q)\right) \quad (17)$$

II.1.2. Algorithms for estimating the volatility-maximizing and level-maximizing trajectories

The purpose of the methodology presented in this subsection consists in computing the trajectory that maximizes a given score function when starting from a given point $\xi_t^{(q)}$, $\forall q \in \mathcal{Q}$, $0 < t \leq T$. In the context of electricity mix robust optimization, we are both interested in the trajectories that respectively maximize or minimize the level of the uncertain parameter and maximize its. As computing the variability and values taken by each possible trajectory would be extremely costly, we provide two algorithms which allow computing exactly the trajectories of quantiles which respectively maximize the level and variability of the uncertain parameter, defined as $\left\{\xi_t^{(q)^H}\right\}_{\substack{q \in \mathcal{Q} \\ 0<t\leq T}}$ and $\left\{\xi_t^{(q)^V}\right\}_{\substack{q \in \mathcal{Q} \\ 0<t\leq T}}$.

The philosophy of the variability-maximizing algorithm can be summarized as follows: for each value of quantile $q \in \mathcal{Q}$ at each point of time, we compute both forward and backward in time the value that maximizes the score function when starting from this value. Starting from $\xi_t^{(q)}$, $0 < t \leq T$, this yields a pair of values $\left(\xi_{t-1}^{(q\prime)}, \xi_{t+1}^{(q\prime\prime)}\right), (q', q'') \in \mathcal{Q}$, from which we compute forward the value that maximizes our function starting from $\xi_{t+1}^{(q\prime\prime)}$, and backward starting from the value $\xi_{t-1}^{(q\prime)}$. By iterating this procedure, we construct a unique trajectory of length T originating from $\xi_t^{(q)}$.

In order to make the presentation of the algorithms as clear as possible, let us start with a certain number of more formal definitions. $\forall q \in \mathcal{Q},\ 0 < t \leq T$, we define η_t^q (resp. ι_{t+1}^q) as the maximum forward variation possible from the value ξ_t^q (resp. the maximum backward variation possible from the value $\xi_{t+1}^{(q)}$). Moreover, we define $\mathrm{H}_t^{\mathfrak{q}_t+}$ (resp. $\mathrm{H}_t^{\mathfrak{q}_t-}$) the maximum (resp. the minimum) forward variation possible, such that $\eta_t^q \in \left\{\mathrm{H}_t^{\mathfrak{q}_t+}, \mathrm{H}_t^{\mathfrak{q}_t-}\right\}$. In order to avoid confusions, we use subscript p when referring to quantile identifier going backward, and q when going forward. The sequences of quantiles corresponding to the variability and level-maximizing trajectories are defined recursively as:

$$\mathfrak{q}_t = \left\{q' \in \mathcal{Q} | \xi_t^{(q\prime)} = \underset{\xi_t \in \mathbb{B}}{\operatorname{argmax}} \left\{ \left\| \xi_t^{(q)} - \xi_{t-1}^{(\mathfrak{q}_{t-1})} \right\| \mid \left\| \xi_t^{(q)} - \xi_{t-1}^{(\mathfrak{q}_{t-1})} \right\| \leq \eta_{t-1}^{\mathfrak{q}_{t-1}}, q \in \mathcal{Q} \right\}\right\} \quad (\mathbf{19})$$

$$\mathfrak{p}_t = \left\{p' \in \mathcal{Q} | \xi_t^{(p')} = \underset{\xi_t \in \mathbb{B}}{\operatorname{argmax}} \left\{ \left\| \xi_t^{(p)} - \xi_{t+1}^{(\mathfrak{p}_{t+1})} \right\| \mid \left\| \xi_t^{(p)} - \xi_{t+1}^{(\mathfrak{p}_{t+1})} \right\| \leq \iota_{t+1}^{\mathfrak{p}_{t+1}}, p \in \mathcal{Q} \right\}\right\} \quad (\mathbf{20})$$

And :

$$\mathfrak{q}_t^H = \left\{q' \in \mathcal{Q} | \xi_t^{(q\prime)} = \sup_{\xi_t \in \mathbb{B}} \left\{ \xi_t^{(q)} | \mathrm{H}_{t-1}^{\mathfrak{q}_{t-1}-} \leq \xi_t^{(q)} - \xi_{t-1}^{\mathfrak{q}_{t-1}^H} \leq \mathrm{H}_{t-1}^{\mathfrak{q}_{t-1}+}, q \in \mathcal{Q} \right\}\right\} \quad (\mathbf{21})$$

In the case we are interest in the level-minimizing trajectory, we just need replacing the supremum by the infimum in the previous expression. The subsets of trajectories generated when using the above described procedure that respectively maximize the variability of the uncertain parameter and its level are defined as:

$$\mathbb{T}^V = \left\{\{(\mathfrak{p}_\tau)_{\tau<t}, q_t, (\mathfrak{q}_{\tau'})_{\tau'>t}\}, \forall q \in \mathcal{Q}, \forall t > 0, t \leq T\right\} \quad (\mathbf{22})$$

$$\mathbb{T}^H = \left\{\left\{q, \left(\mathfrak{q}_{\tau'}^H\right)_{\tau'>1}\right\}, \forall q \in \mathcal{Q},\right\} \quad (\mathbf{23})$$

We define the forward and backward variability scores as:

$$\Omega_{t'\to T}^q = \delta\left(\omega_{t'+1}^q\right) + \sum_{\tau \geq t'+1}^{T-1} \delta\left(\omega_{t+1}^{\mathfrak{q}_t}\right) \quad (\mathbf{24})$$

$$\Omega^{p}_{1\leftarrow t\prime} = \delta\left(\widehat{\omega^{p}_{t\prime-1}}\right) + \sum_{\tau\geq 1}^{t\prime-1} \delta\left(\widehat{\omega^{\mathfrak{p}_{t\prime-\tau}}_{t\prime-\tau-1}}\right) \quad (\mathbf{25})$$

Where

$$\omega^{\mathfrak{q}_{t-1}}_{t} = \underset{\xi_t\in\mathbb{B}}{\operatorname{argmax}}\left\{\left\|\xi^{(q)}_{t} - \xi^{\mathfrak{q}_{t-1}}_{t-1}\right\| \mid \left\|\xi^{(q)}_{t} - \xi^{\mathfrak{q}_{t-1}}_{t-1}\right\| \leq \eta^{\mathfrak{q}_{t-1}}_{t-1}, q\in\mathcal{Q}\right\} \quad (\mathbf{26})$$

$$\omega^{q}_{t} = \underset{\xi_t\in\mathbb{B}}{\operatorname{argmax}}\left\{\left\|\xi^{(q\prime)}_{t} - \xi^{(q)}_{t-1}\right\| \mid \left\|\xi^{(q')}_{t} - \xi^{q}_{t-1}\right\| \leq \eta^{q}_{t-1}, q'\in\mathcal{Q}\right\} \quad (\mathbf{27})$$

$$\widehat{\omega^{\mathfrak{p}_{t+1}}_{t}} = \underset{\xi_t\in\mathbb{B}}{\operatorname{argmax}}\left\{\left\|\xi^{(p)}_{t} - \xi^{\mathfrak{p}_{t+1}}_{t+1}\right\| \mid \left\|\xi^{(p)}_{t} - \xi^{\mathfrak{p}_{t+1}}_{t+1}\right\| \leq \iota^{\mathfrak{p}_{t+1}}_{t+1}, p\in\mathcal{Q}\right\} \quad (\mathbf{28})$$

$$\widehat{\omega^{p}_{t}} = \underset{\xi_t\in\mathbb{B}}{\operatorname{argmax}}\left\{\left\|\xi^{(p\prime)}_{t} - \xi^{p}_{t+1}\right\| \mid \left\|\xi^{(p')}_{t} - \xi^{p}_{t+1}\right\| \leq \iota^{p}_{t+1}, p'\in\mathcal{Q}\right\} \quad (\mathbf{29})$$

With the distance operator δ which measures the absolute variation between two consecutive values, defined as follows:

$$\delta\left(\omega^{\mathfrak{q}_t}_{t+1}\right) = \left\|\underset{\xi_{t+1}\in\mathbb{B}}{\operatorname{argmax}}\left\{\left\|\xi^{(q)}_{t+1} - \xi^{\mathfrak{q}_t}_{t}\right\| \mid \left\|\xi^{(q)}_{t+1} - \xi^{\mathfrak{q}_t}_{t}\right\| \leq \eta^{\mathfrak{q}_t}_{t}, q\in\mathcal{Q}\right\} - \xi^{\mathfrak{q}_t}_{t}\right\| = \left\|\omega^{\mathfrak{q}_t}_{t+1} - \xi^{\mathfrak{q}_t}_{t}\right\| \quad (\mathbf{30})$$

$$\delta\left(\widehat{\omega^{\mathfrak{p}_{t+1}}_{t}}\right) = \left\|\underset{\xi_t\in\mathbb{B}}{\operatorname{argmax}}\left\{\left\|\xi^{(p)}_{t} - \xi^{\mathfrak{p}_{t+1}}_{t+1}\right\| \mid \left\|\xi^{(p)}_{t} - \xi^{\mathfrak{p}_{t+1}}_{t+1}\right\| \leq \iota^{\mathfrak{p}_{t+1}}_{t+1}, p\in\mathcal{Q}\right\} - \xi^{\mathfrak{p}_{t+1}}_{t+1}\right\| = \left\|\widehat{\omega^{\mathfrak{p}_{t+1}}_{t}} - \xi^{\mathfrak{p}_{t+1}}_{t+1}\right\| \quad (\mathbf{31})$$

With $\delta\left(\omega^{q}_{T}\right) = 0$.

Concerning level-maximizing trajectory, it is straightforward that any trajectory that takes highest quantile values more often than all other trajectories maximizes its level. It is thus sufficient to compute only the forward level score, which can be defined as follows:

$$\Theta^{q} = \xi^{(q)}_{1} + \sum_{\tau\geq 1}^{T-1} \theta^{\mathfrak{q}^{H}_{\tau}}_{\tau+1} \quad (\mathbf{32})$$

Where

$$\theta^{\mathfrak{q}^{H}_{t-1}}_{t} = \sup_{\xi_t\in\mathbb{B}}\left\{\xi^{(q)}_{t} \mid \mathrm{H}^{\mathfrak{q}_{t-1}-}_{t-1} \leq \left\|\xi^{(q)}_{t} - \xi^{\mathfrak{q}_{t-1}}_{t-1}\right\| \leq \mathrm{H}^{\mathfrak{q}_{t-1}+}_{t-1}, q\in\mathcal{Q}\right\} \quad (\mathbf{33})$$

In the case we are interested in computing the level-minimizing trajectory again, we just need replacing the supremum by the infimum in equation **(33)**. We define the subsets $\mathcal{A}_{q,t+1}\subseteq\mathcal{Q}$ which include all antecedents of $\xi^{(q)}_{t+1}$, ie all elements $q'\in\mathcal{Q}$ such that $\xi^{(q)}_{t+1} = \operatorname{argmax}_{\xi_{t+1}\in\mathbb{B}}\left\{\left\|\xi^{(q)}_{t+1} - \xi^{(q\prime)}_{t}\right\| \mid \left\|\xi^{(q)}_{t+1} - \xi^{(q\prime)}_{t}\right\| \leq \eta^{q'}_{t}\right\}$. We note the following equivalence, $\forall t\geq 1$:

$$\iota_{t+1}^{p} = \sup\left\{\left\{\bigcup_{q\in\mathcal{A}_{p,t+1}} \eta_t^q\right\} \cup \sup\left\{\left\|\xi_{t+1}^{(p)} - \xi_t^{(q')}\right\| \mid q' \in \mathcal{Q}\backslash\mathcal{A}_{p,t+1}, \left\|\xi_{t+1}^{(p)} - \xi_t^{(q')}\right\| \leq \eta_t^{q'}\right\}\right\} \quad (34)$$

This equivalence simply states that ι_{t+1}^{p} is either equal to the supremum of the absolute distance from the antecedents of $\xi_{t+1}^{(p)}$ or the supremum of the absolute distance from all values such that $\xi_{t+1}^{(p)}$ is not the furthest value which is feasible from $\xi_t^{(q')}, q' \in \mathcal{Q}$. In a similar fashion, we define the subsets $\mathcal{P}_{q,t} \subseteq \mathcal{Q}$ including all elements $q' \in \mathcal{Q}$ such that $\xi_t^{(q)} = \text{argmax}_{\xi_t\in\mathbb{B}}\left\{\left\|\xi_{t+1}^{(q')} - \xi_t^{(q)}\right\| \mid \left\|\xi_{t+1}^{(q')} - \xi_t^{(q)}\right\| \leq \iota_{t+1}^{q'}\right\}$.

As $\forall t > 0, \bigcup_{q\in\mathcal{Q}} \mathcal{A}_{q,t+1} = \mathcal{Q}$, we can further deduce that :

$$\sup_{q\in\mathcal{Q}} \iota_{t+1}^{q} = \sup_{q\in\mathcal{Q}}\left\{\left\{\bigcup_{q'\in\mathcal{A}_{q,t+1}} \eta_t^{q'}\right\} \cup \sup\left\{\left\|\xi_{t+1}^{(q)} - \xi_t^{(q'')}\right\| \mid q'' \in \mathcal{Q}\backslash\mathcal{A}_{q,t+1}, \left\|\xi_{t+1}^{(q)} - \xi_t^{(q'')}\right\| \leq \eta_t^{q''}\right\}\right\} = \sup_{q\in\mathcal{Q}} \eta_t^{q} \quad (35)$$

Moreover, for any $t > 0, q \in \mathcal{Q}$, if $\mathcal{A}_{q,t} = \mathcal{P}_{q,t} = \emptyset$, no trajectory takes the value $\xi_t^{(q)}$. Conversely, there exists $q' \in \mathcal{Q}$ such that the trajectory $\{\mathfrak{p}_{t-1}, q'_t, \mathfrak{q}_{t+1}\}$ varies more in absolute terms than the trajectory defined by $\{\mathfrak{p}_{t-1}, q_t, \mathfrak{q}_{t+1}\}$. Similarly, if for any sequence $(q_\tau)_{t\leq\tau\leq t'}, \bigcup_{t\leq\tau\leq t'} \mathcal{A}_{q_\tau,\tau} = \bigcup_{t\leq\tau\leq t'} \mathcal{P}_{q_\tau,\tau} = \emptyset$, there exists a trajectory that varies more in absolute terms than the trajectory $\{q_\tau\}_{t\leq\tau\leq t'}$.

The utility of our iterative approach relies on the fact that any trajectory that is not included in the subset $\mathbb{T}$ cannot be the trajectory that maximizes the variations of the uncertain parameter. This result is summarized in the following theorem with the associated proof:

Theorem: Let $\mathcal{S} = (q_t^o)_{t>0}$ be a sequence of quantile indexes. Then, by denoting $\Omega^{\mathcal{S}}$ the sum of absolute variations of the sequence $\mathcal{S}$, $\mathcal{S} \notin \mathbb{T}^V \iff \Omega^{\mathcal{S}} \leq \sup_{\mathbb{t}\in\mathbb{T}^V} \Omega^{\mathbb{t}}$.

Proof:

Assume $\exists, \mathcal{S} \notin \mathbb{T}$, $\Omega^{\mathcal{S}} > \sup_{\mathbb{t}\in\mathbb{T}^V} \Omega^{\mathbb{t}}$. Then, $\nexists \mathbb{t} = \left\{\left(\mathfrak{p}_\tau\right)_{\tau<t''}, q_{t'}, \left(\mathfrak{q}_{\tau'}\right)_{\tau'>t'}\right\} \in \mathbb{T}^V$ such that the following condition is verified:

$$\left(\sum_{\tau=1}^{t'-1} \left\|\xi_{\tau+1}^{q_{\tau+1}^o} - \xi_\tau^{q_\tau^o}\right\| \leq \sum_{\tau=1}^{t'-1} \iota_{t'-\tau}^{\mathfrak{p}_{t'-\tau}} + \iota_{t'}^{q_{t'}}\right) \cap \left(\sum_{\tau=t'}^{T-1} \left\|\xi_{\tau+1}^{q_{\tau+1}^o} - \xi_\tau^{q_\tau^o}\right\| \leq \sum_{\tau=t'+1}^{T-1} \eta_\tau^{\mathfrak{q}_\tau} + \eta_{t'}^{q_{t'}}\right)$$

Yet, as $\forall t \leq T-1, \forall q \in \mathcal{Q}$, $\left\|\xi_{\tau+1}^{q_{\tau+1}^o} - \xi_\tau^{q_\tau^o}\right\| \leq \sup_{q\in\mathcal{Q}} \eta_t^q = \sup_{q'\in\mathcal{Q}} \iota_{t+1}^{q'}$, the following condition must hold $\forall q \in \mathcal{Q}, \forall t' \leq T-1$:

$$\left(\left(\left(\left\|\xi_{t\prime}^{q_{t\prime}^o}-\xi_{t\prime-1}^{q_{t\prime-1}^o}\right\|\leq\sup_{q\in\mathcal{Q}}\iota_{t\prime}^{q}\right)\cap\left(\left\|\xi_{t\prime+1}^{q_{t\prime+1}^o}-\xi_{t\prime}^{q_{t\prime}^o}\right\|\leq\sup_{q\in\mathcal{Q}}\eta_{t\prime}^{q}\right)\right)\cap\left(\left(\sum_{\tau=t\prime}^{T-1}\left\|\xi_{\tau+1}^{q_{\tau+1}^o}-\xi_{\tau}^{q_{\tau}^o}\right\|>\sum_{\tau=t\prime+1}^{T-2}\eta_{\tau}^{\mathfrak{q}_\tau}+\eta_{t\prime}^{q_{t\prime}}\right)\cap\left(\sum_{\tau=1}^{t\prime-1}\left\|\xi_{\tau+1}^{q_{\tau+1}^o}-\xi_{\tau}^{q_{\tau}^o}\right\|>\sum_{\tau=1}^{t\prime-1}\iota_{t\prime-\tau}^{\mathfrak{p}_{t\prime-\tau}}+\iota_{t\prime}^{q_{t\prime}}\right)\right)\right)$$

This implies that for each trajectory $\left\{(\mathfrak{p}_\tau)_{\tau<t\prime},q_{t\prime}^o,(\mathfrak{q}_{\tau\prime})_{\tau\prime>t\prime}\right\}$, there exists a couple (t_1,t_2), $1<t_1\leq t'\leq t_2<T$, such that the two following conditions hold:

$$\left(\left(\sum_{\tau=1}^{t_1-1}\left\|\xi_{t'-\tau+1}^{q_{t'-\tau+1}^o}-\xi_{t'-\tau}^{q_{t'-\tau}^o}\right\|\leq\sum_{\tau=1}^{t_1-1}\iota_{t\prime-\tau}^{\mathfrak{p}_{t\prime-\tau}}+\iota_{t\prime}^{q_{t\prime}^o}\right)\cap\left(\sum_{\tau=t\prime}^{t_2-1}\left\|\xi_{\tau+1}^{q_{\tau+1}^o}-\xi_{\tau}^{q_{\tau}^o}\right\|\leq\sum_{\tau=t\prime+1}^{t_2-1}\eta_{\tau}^{\mathfrak{q}_\tau}+\eta_{t\prime}^{q_{t\prime}^o}\right)\right)\cap\left(\sum_{\tau=t_1}^{t'-1}\left\|\xi_{t'-\tau+1}^{q_{t'-\tau+1}^o}-\xi_{t'-\tau}^{q_{t'-\tau}^o}\right\|>\sum_{\tau=t_1}^{t'-1}\iota_{t\prime-\tau}^{\mathfrak{p}_{t\prime-\tau}}+\iota_{t\prime}^{q_{t\prime}^o}\right)$$

$$\left(\left(\sum_{\tau=1}^{t_1-1}\left\|\xi_{t'-\tau+1}^{q_{t'-\tau+1}^o}-\xi_{t'-\tau}^{q_{t'-\tau}^o}\right\|\leq\sum_{\tau=1}^{t_1-1}\iota_{t\prime-\tau}^{\mathfrak{p}_{t\prime-\tau}}+\iota_{t\prime}^{q_{t\prime}^o}\right)\cap\left(\sum_{\tau=t\prime}^{t_2-1}\left\|\xi_{\tau+1}^{q_{\tau+1}^o}-\xi_{\tau}^{q_{\tau}^o}\right\|\leq\sum_{\tau=t\prime+1}^{t_2-1}\eta_{\tau}^{\mathfrak{q}_\tau}+\eta_{t\prime}^{q_{t\prime}^o}\right)\right)\cap\left(\sum_{\tau=t\prime}^{T-1}\left\|\xi_{\tau+1}^{q_{\tau+1}^o}-\xi_{\tau}^{q_{\tau}^o}\right\|>\sum_{\tau=t\prime}^{T-1}\eta_{\tau}^{\mathfrak{q}_\tau}+\eta_{t\prime}^{q_{t\prime}^o}\right)$$

As the above conditions hold for any sequence of quantiles $\left\{(\mathfrak{p}_\tau)_{\tau<t\prime},q_{t\prime}^o,(\mathfrak{q}_{\tau\prime})_{\tau\prime>t\prime}\right\}$, they imply that $\forall t\geq 1,\left(\mathcal{A}_{q_t^o,t}\neq\emptyset\right)\cap\left(\mathcal{P}_{q_t^o,t}\neq\emptyset\right)$ is true. This further implies that $\mathcal{S}\in\mathbb{T}^V$, so $\Omega^{\mathcal{S}}>\Omega^{\mathbb{t}}$ is impossible and we conclude that there exists no trajectory $\mathcal{S}\notin\mathbb{T}^V$ such that $\forall\mathbb{T}\in\mathbb{t},\Omega^{\mathcal{S}}>\Omega^{\mathbb{t}}$.

Then, by computing all trajectories $\mathbb{t}\in\mathbb{T}^V$, the previous theorem implies that the trajectory $\mathbb{t}^*$ which maximizes the total variability $\Omega^{\mathbb{t}}$ is included in the set $\mathbb{T}^V$. This result avoids the costly computation of the total variability of all possible trajectories of the uncertain parameter.

In order to compute both trajectories, our method first requires replacing each value of the uncertain parameter by its nearest quantile in the empirical distribution of the parameter. The, the sequence of operations that are necessary for computing the variability-maximizing trajectory of quantiles (**Algorithm 1**) can be summarized as follows:

Algorithm 1: 4-step algorithm for variability-maximizing trajectory

1 **Step 1:** For $t=1$ to T, for $q\in\mathcal{Q}$, do**:**
Compute $\Omega_{t\rightarrow T}^{q}$ and $\Omega_{1\leftarrow t}^{q}$;

2 **Step 2:** Using matrixes $\boldsymbol{V}^F$ and $\boldsymbol{V}^B$, compute $\boldsymbol{V}=\boldsymbol{V}^F+\boldsymbol{V}^B$;

3 **Step 3:** Compute the couple $(q^*,t^*)=\text{argmax}_{q\in\mathcal{Q},0<t\leq T}\,\boldsymbol{V}$

4 **Step 4:** Compute $\Omega_{t^\circ\rightarrow T}^{q^\circ}$ and $\Omega_{1\leftarrow t^\circ}^{q^\circ}$ to obtain variability-maximizing sequence of quantiles $\left\{(\mathfrak{p}_\tau)_{\tau<t^\circ},q_{t^\circ}^\circ,(\mathfrak{q}_{\tau\prime})_{\tau\prime>t^\circ}\right\}$

5 **End**

Where $\boldsymbol{V}^F=\left(\Omega_{t\prime\rightarrow T}^{q}\right)_{\substack{q\in\mathcal{Q}\\1\leq t\prime\leq T}}$ and $\boldsymbol{V}^B=\left(\Omega_{1\leftarrow t\prime}^{p}\right)_{\substack{p\in\mathcal{Q}\\1\leq t\prime\leq T}}$. The strategy of this algorithm consists in computing the variability-maximizing trajectory, using the iterative procedure described above, starting

from each quantile of the uncertain parameter for each point of time. The values of $\boldsymbol{V}$ correspond to the total variability of each trajectory included in the subset $\mathbb{T}^V$. Then, the row and column index of the greatest element of $\boldsymbol{V}$ indicate the "origin" point of the variability-maximizing trajectory, which can finally be obtained by computing $\Omega_{t^\circ \to T}^{q^\circ}$ and $\Omega_{1 \leftarrow t^\circ}^{q^\circ}$. The variability-maximizing trajectory is noted $\left\{\xi_t^{(q)^\circ}\right\}_{0<t\leq T}$. Similarly, defining the vector $\boldsymbol{\Theta} = (\Theta^q)_{q\in\mathcal{Q}}$, the sequence of operations required for computing the level-maximizing quantile trajectory (**Algorithm 2**) can be expressed as:

Algorithm 2: 3-step algorithm for level-maximizing trajectory

Step 1: For $q \in \mathcal{Q}$, do**:**
→ Compute $\boldsymbol{\Theta} = (\Theta^q)_{q\in\mathcal{Q}}$;
Step 2: Compute $q^* = \text{argmax}_{q\in\mathcal{Q},}\, \boldsymbol{\Theta}$
Step 3: Compute $\Theta_{t^* \to T}^{q^*}$ to obtain level-maximizing trajectory $\{q_{t^*}^*, (\mathfrak{q}_\tau^L)_{\tau>1}\}$
End

The level-maximizing trajectory is noted $\left\{\xi_t^{(q)^*}\right\}_{0<t\leq T}$. In order to avoid confusion, we further note the level-maximizing trajectory as $\left\{\xi_t^{(q)^{*+}}\right\}_{0<t\leq T}$ and the level-minimizing one as $\left\{\xi_t^{(q)^{*-}}\right\}_{0<t\leq T}$. For a given set $\mathcal{Q}$ with cardinal $|\mathcal{Q}|$ and $T > 0$, the number of possible trajectories of quantile values is equal to $(|\mathcal{Q}| + 1)^T$. The first step of Algorithm 1 requires performing, for each time step, at most $|\mathcal{Q}| + 1$ operations. Thus, as the starting value is known for each step, the computation of matrixes $\Omega_{t' \to T}^q$ and $\Omega_{1 \leftarrow t'}^q$ requires $(T-1)(|\mathcal{Q}|+1)^2$ operations, while the second step requires a maximum of $T(|\mathcal{Q}|+1)$ additions. Finally, deriving the maximum value of matrix $\boldsymbol{V}$ corresponds to at most $T(|\mathcal{Q}|+1)$ operations, and finally $(T-1)(|\mathcal{Q}|+1)$ operations are necessary in order to recompose the variability-maximizing trajectory from the point $\xi_{t^\circ}^{(q^\circ)}$. In total, Algorithm 1 requires exactly $(|\mathcal{Q}|+1)\big((T-1)(|\mathcal{Q}|+1)+2T\big)$, so it has a time complexity of $\mathcal{O}\left((|\mathcal{Q}|+1)\big((T-1)(|\mathcal{Q}|+1)+2T\big)\right)$.

Algorithm 2 has a time complexity of $\mathcal{O}\big((T-1)(|\mathcal{Q}|+1)^2\big)$. Computing the level-minimizing trajectory simply requires replacing $q^* = \text{argmax}_{q\in\mathcal{Q},}\, \boldsymbol{\Theta}$ in **Step 2** by $q^* = \text{argmin}_{q\in\mathcal{Q},}\, \boldsymbol{\Theta}$, which takes the same number of operations. We see both our algorithms are polynomial time algorithms and provide efficient tools for computing extreme trajectories. For $|\mathcal{Q}| = 9$ (taking deciles in the distribution of the parameter) and $T = 24$, Algorithm 1 and 2 respectively require at most 2780 and 2300 operations, while there are 10^{24} possible trajectories.

Replacing $\left(\xi_t^{(q)}\right)_{\substack{q\in\mathcal{Q}\\0<t\leq T}}$ by $\left(\xi_t^{(q)}+\widehat{\beta_q}\right)_{\substack{q\in\mathcal{Q}\\0<t\leq T}}$, $-\beta_q \leq \widehat{\beta_q} \leq \beta_q$, it is possible to estimate the level-maximizing and variability-maximizing trajectories for all distributions included in the ambiguity set $\mathbb{B}$, where the vector $\boldsymbol{\beta}$ is determined by the number of observations in the training dataset and the size of $\mathcal{Q}$. Each value of the uncertain parameter is replaced by its nearest neighbor in the vector $\left(\xi_t^{(q)}+\widehat{\beta_q}\right)_{\substack{q\in\mathcal{Q}\\0<t\leq T}}$ for each time period. We can say that a distribution is unambiguously worse than another distribution if the variability and level scores associated with its variability and level maximizing trajectories are both superior or equal to those obtained from the alternative distribution. However, we leave for further research the derivation of the worst-case distribution of the uncertain parameter, as the comparison of variability and level scores depends on the shape of the cost function.

II.2. Cluster-level ambiguity sets

Let us now reintroduce the subscript i and consider the uncertain vector $\boldsymbol{\xi}_t = (\xi_{1t}, \dots \xi_{it}, \dots, \xi_{It}) \in \prod_i \Xi_{it}$, where $\Xi_{it} = [m_{it}, M_{it}]$ for all $i \in I$. For each component of the uncertain vector $\boldsymbol{\xi}_t$ and state $s_i \in S_i$, it is possible to define a cluster-based ambiguity set. Formally, it can be written as follows:

$$\mathbb{B}_i = \left\{ \xi_{it} \in \Xi_t, t \in T \;\middle|\; \begin{array}{ll} \mathbb{P}\left(\xi_{it} \in \Xi_{it}\right) = 1 & \textbf{(36)} \\ \left|F_{it}^{\leftarrow}(q) - \xi_{it}^{(q)}\right| \leq \beta_{iq} & \textbf{(37)} \\ \left|F_{it}^{\leftarrow}(q,r) - \left(\dot{\xi}_{it}\,\middle|_{\xi_{it-1}=\xi_{it-1}^{(q)}}\right)^{(r)}\right| \leq \alpha_{iqr} & \textbf{(38)} \end{array} \right\}$$

As the computation of joint trajectories may be intractable, we make the hypothesis similar to **Yu & Xu (2015)** that the trajectories among different state, within a given empirically possible combination, are independent. This property is essential in order to be able to derive results and individual trajectories for each component of our uncertain vector. This central assumption is equivalent to saying that for any feasible joint state of nature $s_n = (s_1, \dots, s_I)$ and pair $(i, i') \in I$, $i \neq i'$, the stochastic processes $\{\xi_{it}\}_{t\in T} = (\xi_{i1}, \xi_{i2}, \dots, \xi_{i\tau})$ and $\{\xi_{i't}\}_{t\in T} = (\xi_{i'1}, \xi_{i'2}, \dots, \xi_{i'\tau})$ are independent. The cross correlations between components of $\{\boldsymbol{\xi}_t\}_{t\in T}$ are assumed negligible once controlling for the joint state of nature.

However, it may be objected that this approach may generate unrealistic residual demand trajectories and overly conservative results, by introducing too much variability. Moreover, the bounds on the volatility of each component of $\{\boldsymbol{\xi}_t\}_{t\in T}$ are estimated separately and not as functions of the volatility of other components. Yet, it is possible to hierarchically estimate the matrixes $\left(\eta_{it}^q\right)_{\substack{q\in\mathcal{Q}\\0<t\leq T}}$ and $\left(\iota_{it}^q\right)_{\substack{q\in\mathcal{Q}\\0<t\leq T}}$ as functions of $\left(\eta_{-it}^q\right)_{\substack{q\in\mathcal{Q}\\0<t\leq T}}$ and

$\left(\iota_{-it}^{q}\right)_{\substack{q\in Q \\ 0<t\leq T}}$, where $-i \in I$ correspond to components different from i which optimal trajectories have been estimated in previous steps. Similarly, as the volatility of trajectory is measured for each parameter separately, the volatility of residual demand (seen as a linear combination of electricity demand and production of renewables) may be quite low due to variations "cancelling" each other (an increase in demand may be cancelled out by an increase in wind production at the same period). Again, it is possible to hierarchically estimate $\left\{(\mathfrak{p}_{i\tau})_{\tau<t^\circ}, \mathring{q_{it}}^{\circ}, (\mathfrak{q}_{i\tau'})_{\tau'>t^\circ}\right\}$, where $\left\{(\mathfrak{p}_{i\tau})_{\tau<t^\circ}, \mathring{q_{it}}^{\circ}, (\mathfrak{q}_{i\tau'})_{\tau'>t^\circ}\right\}$ maximizes the volatility of $\{\xi_{it}\}_{t\in T}$ conditional on $\left\{(\mathfrak{p}_{-i\tau})_{\tau<t^\circ}, \mathring{q}_{-it}^{\circ}, (\mathfrak{q}_{-i\tau'})_{\tau'>t^\circ}\right\}$.

If the assumption that individual trajectories are independent within cluster combinations is verified, then it is possible to estimate the worst-case (level and volatility) trajectories for each component of our uncertain vector. Then, assuming that $\{\boldsymbol{\xi_{1t}}\}_{t\in T}$ corresponds to electricity demand parameters and $\{\boldsymbol{\xi_{it}}\}_{t\in T}, i > 1$ to RES capacity factor parameters, we can define residual demand as follows, $\forall t \in T$:

$$\mathcal{R}_t = \xi_{1t} - \sum_{i=2}^{I} C_i \xi_{it} \tag{39}$$

, where C_i corresponds to the installed capacity of RES technology $i > 1$. Recall from II.1. that we defined the worst-case state combinations as $s^{*+} = (s_1^+, s_2^-, \dots, s_I^-)$ and $s^{*-} = (s_1^-, s_2^+, \dots, s_I^+)$. Then, it is possible to express respectively the maximum level, minimum level and maximum volatility trajectories as linear combinations of residual demand components, noted $\{\mathcal{R}_t^H\}_{t\in T}$, $\{\mathcal{R}_t^L\}_{t\in T}$ and $\{\mathcal{R}_t^V\}_{t\in T}$ respectively. We have, $\forall t \in T$:

$$\mathcal{R}_t^H = \xi_{1t}^{(q)^{*+}} - \sum_{i=2}^{I} C_i \xi_{it}^{(q)^{*-}} \tag{40}$$

$$\mathcal{R}_t^L = \xi_{1t}^{(q)^{*-}} - \sum_{i=2}^{I} C_i \xi_{it}^{(q)^{*+}} \tag{41}$$

$$\mathcal{R}_t^V = \xi_{1t}^{(q)^{\circ}} - \sum_{i=2}^{I} C_i \xi_{it}^{(q)^{\circ}} \tag{42}$$

III- Numerical experiment: Electricity mix optimal investment and dispatch under uncertain residual demand

III.1. Presentation and description of the optimization model

The presentation and formulation of variables, parameters and equations is largely borrowed from **De Sisternes (2013)** as it provides great readability to the model and facilitates the understanding of equations. For saving some space, the full formulation of the model, including description of parameters, variables and equations, is provided in the Appendix.

The model used for this numerical experiment is formulated as a MILP (Mixed-Integer Linear Programming) with unit commitment and transmission constraints. We include constraints on ramping up and down of production units, maximum and minimum stable output levels, minimum up and down times, online or offline status, in addition to flow balance and flow capacities constraints for the network. We include storage devices under the form of batteries, reservoirs and hydraulic pumped storage stations, and electric vehicles (EVs) which are modeled as batteries with an hourly minimum state-of-charge requirement based on the expected distance driven in the following time period. Finally, we include constraints on CO2 price, in addition to supply-demand equilibrium constraints corresponding to both level-maximizing and volatility-maximizing residual demand trajectories. The model is formulated at the regional geographical scale, while combining yearly, seasonal and hourly time scales.

III.2. Technical assumptions

In the following section, we present the results of the model described above applied in the case of the French region Auvergne Rhône-Alpes. This administrative region is located in the South-East of France and enjoys strong solar irradiation compared to the national average. In addition, it accounts for roughly 11.6% of French GDP, while its mean share of national electricity load equals to 13.8%.

We assume no initial generation capacities in order to better disentangle the impact of each worst-case trajectories on investment decisions. For convenience, we further assume that no investment occurs in hydroelectric production units and keep the number of EVs to 0. As only one region is considered, transmission constraints and transmission costs are not included in the estimated model. Moreover, we constrain the variable for capacity investment to take only discrete values for nuclear, gas turbines (GT) and combined cycle gas turbine plants (CCG), and continuous values for other production and storage technologies. Nuclear investment is performed by blocks of 1.6 GW, corresponding to the rated power of the EPR Flamanville plant (the most recent nuclear power project in France), while CCG investments are made by blocs of 0.45 GW, which corresponds to the average nominal power of General Electric's 9HA.01/.02 gas turbine. Finally, GT investments are performed by blocks of 0.3 GW. Flexibility characteristics of main generation units can be found in **Table** 1. Oil and gas prices are forecasted using

linear regression, we take Netherlands TTF and OECD countries CIF per million Btu dollar prices as reference on the period 2005-2018[1]. Finally, we take a 5% discount rate and a CO2 price equal to 50€/ton, without taking any CO2 emission ceiling. Investments decisions are made for the year 2021.

Technology	Minimum Load (% nominal power)	Ramping rate (% of nominal power/min)	Minimum uptime/downtime (hours)
Combined cycle gas turbine	45	20	0
Oil turbine	20	8	2
Nuclear	50	2-5	10
Hydroelectric	5	15	0.1

Table 1: Flexibility characteristics of main generation technologies.

Sources: Gonzalez-Salazar et al. (2018), IAEA (2018), Schill et al. (2016), IEA (2015), Schröder et al. (2013), EC JRC (2010).

In order to simplify the practical application of the methodology presented in section II, we use the theoretical worst-case joint state of nature (s^{*+}, s^{*-}) instead of the empirical one $(\hat{s}^{+}, \hat{s}^{-})$. Yet, this assumption may generate trajectories significantly more variable than empirically observed ones, which may lead to overly conservative investment decisions. Thus, we compare the results using residual demand trajectories generated using Algorithms 1 and 2 with empirically observed worst-case residual demand trajectories. For convenience, we let the reader refer to the Appendix for detailed explanations on the estimation of empirically observed worst-case trajectories.

When considering the technical characteristics of generation technologies presented in **Table 1**, one actually notice that ramping rates are high enough for each technology units to vary their output within their entire production range. Indeed, as the model is defined using hourly time step, nuclear plants may vary their production by up to 100% of their rated power within an hour. Thus, ramping constraints are not binding within hourly time resolution. Moreover, when looking at dispatch data from RTE, it appears that nuclear plants especially are operated with much less flexibility than their technical characteristics actually allow. Taking national hourly production data on the period 2013-2018, **Figure 1** shows the distribution of the rate of variation of nuclear output, defined with respect to nominal power:

[1] See BP Statistical Review of World Energy, June 2019

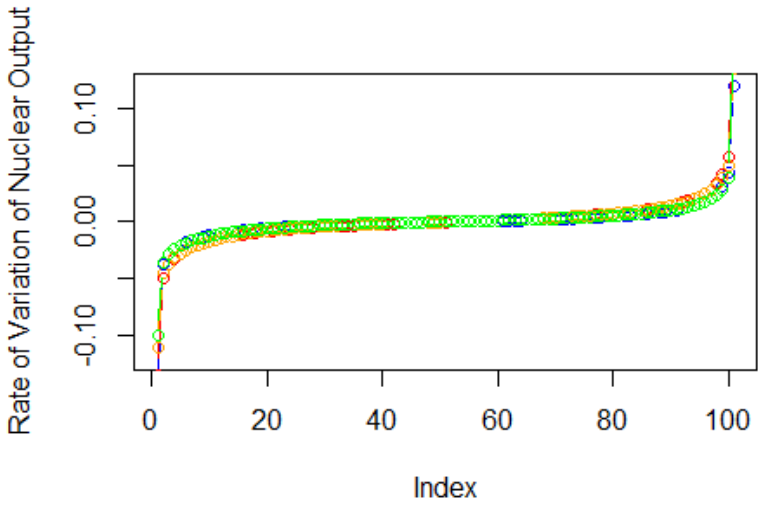

Figure 1: Percentile distribution of the hourly rate of variation for nuclear power (right)

Note: The distributions are reported for each season as RD patterns change seasonally. Blue, red orange and green respectively correspond to distributions for winter, spring, summer and autumn. The horizontal axis corresponding to percentiles of the distribution of variations.

It appears from **Figure 1** that in roughly 90% of cases, nuclear output hourly variations are comprised within -2.1% and +2.1%. If we take the whole distribution, the lower an upper bounds on hourly variations observed in the data become -12.4% and +13.9%. Still, these figures remain largely inferior to the ramping capacities of nuclear units, which suggests they are operated in a much rigid way considering their flexibility characteristics. This directly relates to the fact that RTE[2] uses nuclear plants for baseload production instead of load-following.

A similar reasoning may be carried out for all technologies. We here focus on the case of nuclear, and add these operational "rules" as constraints to our optimization model. In order to precisely analyze how operational flexibility affects investment decisions, we include the minimum and maximum hourly variation values as operational bounds for thermal units.

[2] RTE is the French transmission system operator

III.3. Numerical simulation results

We start by analyzing the investment results obtained when using trajectories obtained using both Algorithms 1 and 2, that are presented in **Table 2**. As we assume no initial installed capacities, the figures reported correspond to the level of generation capacity for each technology in 2021, using successively theoretical worst-case RD trajectories and empirical trajectories. For each column, the figures on the left correspond to the optimal investment level with maximum-level-robust only decisions, while figures on the right correspond to both maximum-level-robust and variability-robust decisions. We provide in Appendix optimal investment results when taking simultaneously minimum-level-robust, maximum-level-robust and variability-robust decisions. As the variability of solar and wind capacity factors would have no effect on the shape of residual demand for null installed capacities, we impose various thresholds values for the level of investment in renewable technologies.

	> 1 GWe		**> 3 GWe**		**> 5 GWe**	
	TT	ET	TT	ET	TT	ET
Combined cycle gas turbine	4.05/8.1	4.95/5.85	4.05/9.9	4.95/6.75	4.05/10.8	5.85/6.75
Gas turbine	1.2/1.2	1.2/1.8	1.2/0.6	0.9/2.4	1.2/0.9	0.9/2.1
Nuclear	19.2/12.8	17.6/16	19.2/11.2	17.6/14.4	19.2/9.6	16/14.4
Wind	0/0	0.52/0	0/0	0.064/0	0/0.33	0.30/1.07
Utility-scale PV	1/1	1.21/1	3/3	2.93/3	5/4.67	4.70/3.93
Commercial PV	0/0	0/0	0/0	0/0	0/0	0/0
Residential PV	0/0	0/0	0/0	0/0	0/0	0/0
Battery storage	1.40/9.89	3.70/2.73	2.41/10.40	5.51/6.40	2.89/10.73	6.55/3.50

Table 2: Optimal investment level by technology, with constraints on minimum installed capacities for renewables (TT= Theoretical trajectories only)

It can first be noted from **Table 2** that as the threshold for renewables installed capacities increases, the investments in peaking technologies (CCG and gas turbines) are non-decreasing for all cases, while the capacities in nuclear decrease. Yet, while in the level-robust only case, investment in peaking technologies remain constant with respect to the threshold value, the sum of their installed capacities is always increasing with level-variability robustness (especially using theoretical trajectories). The behavior of investment in batteries is more chaotic: as its optimal level steadily increases both for level-robust only and level-variability-robust investment decisions using theoretical trajectories, its level-robust capacities increase while its level-variability-robust capacities decrease using empirical trajectories.

When hedging against both types of worst-case trajectories, peaking technologies and battery storage seem to behave as substitutes in the empirical case and complements in the theoretical case. This complementarity can be explained by the fact that, while higher capacities in battery storage allow the smoothing of highly variables renewable production when capacities increase, thermal peaking technologies remain necessary as the capacity factors of wind and solar units is quasi null in the level-maximizing RD trajectory. Theoretical trajectories may thus result in slight over conservatism compared to empirical ones. Indeed, as level-robust only investment levels obtained using theoretical and empirical trajectories are quite close, this indicates level-maximizing trajectories have similar profiles while the theoretical variability-maximizing trajectory exhibits significantly higher variability than the empirical one. High storage capacities are thus necessary for high variability periods, yet the equilibrium of the electric system still requires significant thermal capacities for high residual demand periods.

> 1 GWe	Adapted mix (TT)	Non-adapted mix (TT)	Adapted mix (ET)	Non-adapted mix (ET)
Yearly fixed costs & annuities (M€)	5254	6907	6000	6583
Variable costs (level-maximizing week) (M€)	112.96	61.02	76.90	60.18
Variable costs (variability-maximizing week) (M€)	43.23	INF	45.81	34.78
> 3 GWe				
Yearly fixed costs & annuities (M€)	4965	7067	5779	6668
Variable costs (level-maximizing week) (M€)	119.31	60.21	94.03	59.88
Variable costs (variability-maximizing week) (M€)	101.46	INF	52.93	34.47
> 5 GWe				
Yearly fixed costs & annuities (M€)	4665	7213	5911	6370
Variable costs (level-maximizing week) (M€)	134.25	59.75	84.54	70.52
Variable costs (variability-maximizing week) (M€)	56.49	INF	49.17	40.48
> 10 GWe				
Yearly fixed costs & annuities (M€)	4660	7611	5940	7053
Variable costs (level-maximizing week) (M€)	155.32	59.44	94.59	58.70
Variable costs (variability-maximizing week) (M€)	54.18	INF	47.82	27.05

Table 3: Cost decomposition of the electricity mix, with constraints on minimum installed capacities for renewables (INF= Infeasible dispatch, TT only)

As shown in **Table 3**, the adapted mix, corresponding to level-variability robust investment decisions, systematically exhibit lower yearly fixed cost and annuities than the non-adapted mix, corresponding to the level-only robust decision. Similarly, the adapted mix always has higher variable costs, both in the case of the level-maximizing and variability-maximizing weeks, compared to the non-adapted one. However, the theoretical variability-maximizing week is always integer infeasible with the non-adapted mix, even when allowing curtailment of renewables and load shedding, which would result in a system blackout. Yet, the empirical variability-maximizing week remains feasible with the non-adapted mix and at least cost than with the adapted mix. Apart from the theoretical case, we observe a clear trade-off between high variable costs and low fixed costs mixes depending on targeted level of system flexibility.

Yet, both adapted and non-adapted mixes exhibit a high share of CO2 emitting production capacities, which would result in highly polluting and expensive mixes depending on the price of carbon. After measuring that a higher CO2 price doesn't significantly change the above results, we impose a restriction on the maximum number $A \in \mathbb{N}^*$ of oil and gas power plants in the mix. This ceiling is defined such that the optimization problem is infeasible for any number of fossil plants strictly lower than A. In other words, A corresponds to the minimum number of oil and gas production units necessary to maintain the frequency of the electric system within acceptable bounds without using reserves. The resulting production mixes and cost decomposition are presented in **Table 4** and **Table 5** respectively

	> 3 GWe		**> 5 GWe**	
	TT	ET	TT	ET
Combined cycle gas turbine	0/9	0/4.05	0/9	0/4.5
Gas turbine	0/0	0.9/0	0/1.2	0.9/0
Nuclear	24/12.8	20.8/17.8	24/11.2	20.8/17.6
Wind	0/0.3	5.56/1.53	0/0	5.74/0.9
Utility-scale PV	3/2.7	0/1.47	5/5	0/4.1
Commercial PV	0/0	0/0	0/0	0/0
Residential PV	0/0	0/0	0/0	0/0
Battery storage	13.76/20.4	19.51/23.8	13.51/18.8	18.78/12.8

Table 4: Optimal investment level by technology, with constraints on minimum installed capacities for renewables and maximum on CO2 emitting power plants

While CO2 emitting technologies completely disappear from the non-adapted mixes, both for theoretical and empirical trajectories, **Table 4** exhibits much higher battery storage capacities for adapted mixes compared to **Table 2**, with an incompressible level of oil and gas plants only slightly lower than for unconstrained investment. With a minimum level of 3 GWe of renewable capacities, the TT adapted mix

has 96 % higher battery storage capacities while roughly 16% lower oil and gas production capacities compared to **Table 2**, while these ratios to expand to 372% and 56% respectively for the ET adapted mix. A similar observations can be made when imposing a minimum of 5 GWe of renewables in the mix. The flexibility "loss" of not investing 1 GWe of oil or gas production unit in the system must be compensated by more than 6 GWe of battery storage to ensure an equivalent level of system flexibility.

As observed in **Table 5**, this results into significantly higher yearly fixed costs and annuities for both adapted and non-adapted mixes. For a threshold of 3 GWe, TT and ET adapted mixes respectively exhibit 15% and 24% higher yearly FOM costs and annuities compared to **Table 3**, while these ratios decrease to 13% and 18% respectively for a threshold of 5 GWe of renewables.

> 3 GWe	Adapted mix (theoretical)	Non-adapted mix (theoretical)	Adapted mix (empirical)	Non-adapted mix (empirical)
Yearly fixed costs & annuities (M€)	5718	8675	7189	8401
Variable costs (level-maximizing week) (M€)	103.30	25.17	55.20	38.83
Variable costs (variability-maximizing week) (M€)	37.25	INF	29.66	INF
> 5 GWe				
Yearly fixed costs & annuities (M€)	5283	8802	7006	8409
Variable costs (level-maximizing week) (M€)	129.54	25.15	55.52	33.98
Variable costs (variability-maximizing week) (M€)	95.61	INF	30.24	INF

Table 5: Cost decomposition of the electricity mix, with constraints on minimum installed capacities for renewables and maximum on CO2 emitting power plants

Similar conclusions can be drawn when comparing minimum-maximum-level-robust to minimum-maximum-level-robust and variability-robust decisions with empirical data. Investment results and costs figures are reported in **Table 6** and **7** in Appendix. However, we made the assumption that there are no initial capacities. In the case preexisting capacities are not retired when new investments are made, increasing the share of renewables in the electric mix increases more than proportionally the total FOM costs and annuities of the system. As increasing decarbonization imposes increasingly avoiding CO2 emitting technologies, the total costs of the system will increase more rapidly than the share of renewables because of increasing investments in storage for flexibility requirement. In the case the electric mix is not properly designed in terms of flexibility needs (non-adapted mix), the objective of minimizing CO2 emissions while developing renewables may trigger infeasible situations resulting in system blackouts with extremely high costs for the society.

IV- Conclusion

We presented in this paper an original approach based on philosophy of DRO and the tools of RO in order to derive worst-case trajectories of uncertain parameters, derived both in terms of level *and* variability. As a higher share of renewables in the electricity mix is associated with higher residual demand variability, it makes sense to hedge against situations that would require high flexibility from the system and push power plants to their technical limits.

For each possible matrix of quantile values for the uncertain parameter defined in the *trajectory ambiguity set*, we derive its level-maximizing and variability-maximizing trajectories expressed in quantiles of its empirical distribution. For each value of this matrix, it is possible to derive a pair of trajectories and thus a joint distribution of worst-case trajectories associated to each possible value of the vector $\boldsymbol{\beta}$ described in Section 2. We leave the derivation of the worst-case theoretical probability distribution of the uncertain parameter based on this joint distribution for further research. Still, we prove how our simple framework can be used for refining utility investment decisions in the context of the transition of electric systems, allowing us to derive optimal solutions hedging against situations of extremely levels and variability of uncertain parameters at minimum cost.

Appendix:

Appendix to III.1.:

The presentation and formulation of variables, parameters and equations is largely borrowed from **De Sisternes (2013),** as it provides great readability to the model and facilitates the understanding of equations.

III.1.1. Indices and sets

$j \in \mathcal{J}$, where $\mathcal{J}$ is the set of electricity generation technologies
$\mathcal{T} \subset \mathcal{J}$, where $\mathcal{T}$ is the subset of thermal generation technologies
$\mathcal{W} \subset \mathcal{J}$, where $\mathcal{W}$ is the subset of wind power generation technologies
$\mathcal{P} \subset \mathcal{J}$, where $\mathcal{P}$ is the subset of solar generation technologies
$\mathcal{B} \subset \mathcal{J}$, where $\mathcal{B}$ is the subset of storage technologies
$r \in \mathcal{R}$, where $\mathcal{R}$ is the set of geographical regions
$y \in \mathcal{Y}$, where $\mathcal{Y}$ is the set of years
$s \in \mathcal{S}$, where $\mathcal{S}$ is the set of seasons
$h \in \mathcal{H}$, where $\mathcal{H}$ is the set of hours
$\mathfrak{t} \in \mathfrak{T}$, where $\mathfrak{T}$ is the set of worst-case trajectories

The sets used in the model can be classified into two types: sets and subsets related to production and storage technologies and sets related to various temporal and geographical scales. $\mathcal{J}$ corresponds to the set of available generation and storage technologies that can be built. It can be decomposed into subsets, each corresponding to varieties of technologies: $\mathcal{W}$ and $\mathcal{P}$ respectively denote wind and solar generation technologies , while $\mathcal{T}$ refers to the subset of thermal power units, including in our case combined cycle gas turbines (CCGT), fuel turbines, coal and nuclear technologies.

$\mathcal{H}$ corresponds to the set of hours in a week as we model investment and dispatching decisions with an hourly time resolution. Our model thus combines multiple time scales in order to both account for long-term and short-term constraints which determine investment and dispatching decisions. As we model cyclical stochastic processes, the distributions of parameters $\xi_{rysh}$and ξ_{rysh+P} are identical. Note that when referring to the distribution of ξ_{rysh}, we actually refer to the distributions of $\{\xi_{rysnP}\}_{\tau\in[0,P]}, 0 \leq n \leq N$.

III.1.2. Parameters

$\mathcal{R}^{\mathfrak{t}}_{rysh} \in \mathbb{R}$: residual demand for trajectory $\mathfrak{t}$ in region r, year y, season s and hour h [MW]

$c^{I}_{jy} \in \mathbb{R}^{+}$: investment cost for technology j in year y [€/MWe]

$A_{jy} \in \mathbb{R}^{+}$: annuity paid for investment in technology j made in year y [€/MWe/year]

$c^{FOM}_{jy} \in \mathbb{R}^{+}$: annual fixed operation & management costs for technology j in year y [€/MWe]

$c^{V}_{jy} \in \mathbb{R}^{+}$: variable cost for technology j in year y [€/MW]

$c^{STUP}_{jy} \in \mathbb{R}^{+}$: start-up cost for technology j in year y [€]

$c^{L}_{y} \in \mathbb{R}^{+}$: investment cost for a transmission line in year y [€/km]

$A^{L}_{y} \in \mathbb{R}^{+}$: annuity paid for investment in a transmission line made in year y [€/km/year]

$c^{L,FOM}_{y} \in \mathbb{R}^{+}$: annual fixed operation & management cost for transmission line in year y [€/MW]

$VOLL$: value of lost load [€/MW]

O_{jr}: initial capacity level for technology j in region r [MWe]

$O^{L}_{rr\prime}$: initial transmission capacity between regions r and r' [MW]

$\overline{q_j}$: maximum output level for production technology j [%]

$\underline{q_j}$: minimum stable power output level for technology j [%]

$\overline{r_j}$: maximum ramp-up capability for technology j [MW/h]

$\underline{r_j}$: maximum ramp-down capability for technology j [MW/h]

M^{U}_{j}: minimum up-time for technology j [h]

M^{D}_{j}: minimum down-time for technology j [h]

E_j: CO2 emissions per unit output for technology j [ton/MW]

η_j: round-trip efficiency for storage technology $j \in \mathcal{B}$ [%]

$\overline{\mathrm{B}_j}$: maximum state of charge for storage technology j [%]

$\underline{\mathrm{B}_j}$: minimum state of charge for storage technology j [%]

η^{EV}_{j}: round-trip efficiency for electric vehicles [%]

$\overline{\mathrm{B}^{EV}}$: maximum state of charge for electric vehicles [%]

$\underline{\mathrm{B}^{EV}}$: minimum state of charge for electric vehicles [%]

$\phi_{[h,h+1]} \in \mathbb{R}^{+}$: average distance driven between hours h and $h+1$ [km]

$k^{EV} \in \mathbb{R}^{+}$: per kilometer electric consumption of electric vehicles [MW/km]

$NV_{ry} \in \mathbb{N}$: total number of vehicles in region r and year y

α^{EV}_{ry}: share of electric vehicles in total vehicle fleet in region r and year y [%]

$d_{rr\prime}$: distance between the centroids of regions r and r' [km]

$\overline{E_y}$: limit on CO2 emissions for year y [Mtons]

p_y^{CO2}: price of CO2 carbon ton in year y [€/ton]

$\beta \in \mathbb{R}^+$: discount rate [%]

$\tau \in \mathbb{R}^+$: additional transmission capacity for each new transmission line [MW]

$\Omega \in \mathbb{R}^+$: slack parameter

$\rho \in [10^{-3}, 10^{-2}]$: frequency primary control tuning parameter

$D^{lim} \in \mathbb{R}^+$: frequency deviation absolute limit

As our model allows investment in transmission capacity, cost parameters can be divided between generation costs (investment costs expressed in annuities, maintenance costs, variable and start-up costs) and transmission network costs (investment costs expressed as annuities, maintenance costs). We make the assumption that the variable cost of transmitting electricity is equal to zero. Finally, we define the value of lost load (VOLL), which corresponds to the cost of one non-served unit of electricity demand.

We introduce generation units technical constraints, including maximum and minimum stable power output (the latter applying when a unit is online, ie effectively feeding electricity into the network), ramping up and down limits and minimum up and down times, in addition to CO2 emission rate, for each technology. Specifically for storage technologies and electric vehicles (EV), we consider maximum and minimum state of charge limits, charging speed, round-trip efficiency (we choose $\eta_j = \eta_j^{EV} = 90\%$), in addition to the average number of kilometers for each time interval of the day in order to approximate the electricity consumption requirements of an EV fleet.

Finally, we introduce distance measures for each arc $r - r'$, where its length is calculated as the distance in kilometers between the centroids of regions r and r'. This provides an approximation for the length of new transmission lines to build for reinforcing transmission capacities along arc $r - r'$. Yet, we may consider the resulting investment costs as upper bounds as centroid distance is likely to overestimate the length of new lines needed to link the two regions.

III.1.3. Variables

$U_{jry} \in \mathbb{R}^+$: investment level in technology j in region r and year y [MWe]

$U^L_{rr'y} \in \mathbb{N}$: investment in new transmission lines between regions r and r' in year y [MW]

$C_{jry} \in \mathbb{R}^+$: installed capacity of technology j in region r and year y [MWe]

$f_{rr'y}$: transmission capacity between regions r and r' in year y [MW]

$q_{jrysh} \in \mathbb{R}^+$: output power of generation technology j plants in region r, year y, season s and hour of the week h [MW]

$\omega^1_{jrysh} \in \mathbb{R}^+$: auxiliary variable for output power over minimum output of generation technology j plants in region r, year y, season s and hour of the week h [MW]

$\omega^2_{jrysh} \in \mathbb{R}^+$: auxiliary variable for minimum output of generation technology j plants in region r, year y, season s and hour of the week h [MW]

$s_{jrysh} \in \mathbb{R}^+$: slack variable for generation constraints of generation technology j plants in region r, year y, season s and hour of the week h

$R_{rr'ysh} \in \mathbb{R}$: volume of electricity transferred from region r to region r' using arc $r - r'$ [MW]

$\kappa_{jrysh} \in \mathbb{R}^+$: volume of curtailed electricity for wind generation technology j [MW]

$\chi_{rysh} \in \mathbb{R}^+$: volume of non-served electricity [MW]

$\Delta^+_{jrysh} \in \mathbb{R}^+$: electricity inflow from network to storage units of technology j [MW]

$\Delta^-_{jrysh} \in \mathbb{R}^+$: electricity outflow to network from storage units of technology j [MW]

$B_{jrysh} \in \mathbb{R}^+$: state of charge of storage units of technology j [MW]

$\Delta^{EV}_{rysh}{}^+ \in \mathbb{R}^+$: electricity inflow from network to electric vehicles [MW]

$\Delta^{EV}_{rysh}{}^- \in \mathbb{R}^+$: electricity outflow to network from electric vehicles [MW]

$B^{EV}_{rysh} \in \mathbb{R}^+$: state of charge of electric vehicles [MW]

$u_{jrysh} \in \{0,1\}$: commitment state of plants of generation technology j

$z_{jrysh} \in \{0,1\}$: start-up decision of plants of generation technology j

$v_{jrysh} \in \{0,1\}$: shut-down decision of plants of generation technology j

$l_{jrysh} \in \{0,1\}$: charging/discharging state of storage units of technology j

$l^{EV}_{rysh} \in \{0,1\}$: charging/discharging state of electric vehicles

Our model is a MILP (Mixed Integer Linear Program), thus including both positive variables defined of $\mathbb{R}^+$, integer and binary variables. For simplicity, we consider investment and installed levels as continuous variables, while investment in new transmission lines is an integer variable equal to the number of new lines built. Transmission capacity and output power are considered as continuous positive variables as well.

In order to keep our model linear, we introduce two auxiliary variables for production in additional to the slack variable s_{jrysh}. ω^1_{jrysh} is equal to the output power produced by technology j plant in addition to the minimum production level ω^2_{jrysh} . Put differently, the total output power of generation technology j plants is equal to the sum of ω^1_{jrysh} and ω^2_{jrysh}.

The volume of electricity transmitted from region r to region r' is not a decision variable in the model, but is necessary in order to express flow balance and flow capacity constraints. The following variables correspond to the level of curtailed wind power and non-served electricity, storage units and EV stock

(state of charge) and flow. Finally, we introduce binary variables which correspond to the commitment state and start-up/shut-down decision of power plants, in order to account for the physical limitations of thermal and hydropower technologies and mechanical inertia. Finally, the two binary variables l_{jrysh} and l^{EV}_{jrysh} translate the fact that storage units and EV cannot be storing and releasing electricity at the same moment, and can only execute one of those two actions.

III.1.4. Structure of the centralized cost minimization optimization model

$$\min_{\boldsymbol{U},\boldsymbol{U^L},\boldsymbol{q},\boldsymbol{z},\boldsymbol{\chi}} \sum_{y\in\mathcal{Y}} \frac{1}{(1+\beta)^y}\Bigg(\sum_{r\in\mathcal{R}}\Bigg(\sum_{y'\le y}\sum_{j\in\mathcal{J}}\left(A_{jy'} + c^{FOM}_{jy'}\right)U_{jry'} + \frac{\vartheta}{|\mathfrak{T}|}\sum_{s\in\mathcal{S}}\sum_{h\in\mathcal{H}}\sum_{\mathrm{t}\in\mathfrak{T}}\Bigg(\sum_{j\in\mathcal{J}}\left(\left(c^{V}_{jy} + p^{CO2}_{y}E_j\right)q_{jrysh} + c^{STUP}_{jy}z_{jrysh}\right) + VOLL\chi_{rysh}\Bigg) + \sum_{\substack{r'\in\mathcal{R}\\ r'\neq r}}\sum_{y'\le y}\frac{A^L_{y'} + c^{L,FOM}_{y'}}{2}U^L_{rr'y'}\Bigg)\Bigg) \quad (\mathbf{43})$$

s.t.

$$\left|\rho\sum_{r\in\mathcal{R}} {q^{+}_{rysh}}^{\mathrm{t}}\right| \le D^{lim} \qquad ,\forall y\in\mathcal{Y},\forall s\in\mathcal{S},\forall h\in\mathcal{H},\mathrm{t}\in\mathfrak{T} \quad (\mathbf{44})$$

$$\sum_{\substack{r'\in\mathcal{R}\\ r'\neq r}} R_{rr'ysh} - \sum_{\substack{r'\in\mathcal{R}\\ r'\neq r}} R_{r'rysh} = {q^{+}_{rysh}}^{\mathrm{t}} \qquad \forall r\in\mathcal{R},\forall y\in\mathcal{Y},\forall s\in\mathcal{S},\forall h\in\mathcal{H} \ (\mathbf{45})$$

Where:

$${q^{+}_{rysh}}^{\mathrm{t}} = \sum_{j\in\mathcal{J}} q_{jrysh} + \chi_{rysh} + \sum_{j\in\mathcal{B}}\Delta^{-}_{jrysh} + {\Delta^{EV}_{rysh}}^{-} - \mathcal{R}^{\mathrm{t}}_{rysh} - \sum_{j\in\mathcal{B}}\Delta^{+}_{jrysh} - {\Delta^{EV}_{rysh}}^{+} - \kappa_{jrysh}, \forall r\in\mathcal{R},\forall y\in\mathcal{Y},\forall s\in\mathcal{S},\forall h\in\mathcal{H},\forall \mathrm{t}\in\mathfrak{T}$$

$$\left|R_{rr'ysh}\right| \le f_{rr'y'} \qquad ,\forall r\in\mathcal{R},\forall r'\in\mathcal{R},r\neq r',\forall y\in\mathcal{Y},\forall s\in\mathcal{S},\forall h\in\mathcal{H} \ (\mathbf{46})$$

$$C_{jr1} = O_{jr} + U_{jr1} \qquad ,\forall j\in\mathcal{J},\forall r\in\mathcal{R} \ (\mathbf{47})$$

$$C_{jry} = C_{jry-1} + U_{jry} \qquad ,\forall j\in\mathcal{J},\forall r\in\mathcal{R},\forall y\in\mathcal{Y} \ (\mathbf{48})$$

$$f_{rr'1} = O^L_{rr'} + \tau U^L_{rr'1} \qquad ,\forall r\in\mathcal{R},\forall r'\in\mathcal{R},r\neq r' \ (\mathbf{49})$$

$$f_{rr'y} = f_{rr'y-1} + \tau U^L_{rr'y} \qquad ,\forall r\in\mathcal{R},\forall r'\in\mathcal{R},r\neq r',\forall y\in\mathcal{Y} \ (\mathbf{50})$$

$$u_{jrysh} - u_{jrysh-1} = z_{jrysh} - v_{jrysh} \qquad ,\forall j\in\mathcal{J},\forall r\in\mathcal{R},\forall y\in\mathcal{Y},\forall s\in\mathcal{S},\forall h\in\mathcal{H} \ (\mathbf{51})$$

$$z_{jrysh} + v_{jrysh} \le 1 \qquad ,\forall j\in\mathcal{J},\forall r\in\mathcal{R},\forall y\in\mathcal{Y},\forall s\in\mathcal{S},\forall h\in\mathcal{H} \ (\mathbf{52})$$

$$\omega^1_{jrysh} = q_{jrysh} - \omega^2_{jrysh} \quad ,\forall j \in \mathcal{J}, \forall r \in \mathcal{R}, \forall y \in \mathcal{Y}, \forall s \in \mathcal{S}, \forall h \in \mathcal{H} \ (\mathbf{53})$$

$$\omega^1_{jrysh} - \omega^1_{jrysh-1} \leq \overline{r_j} \quad ,\forall j \in \mathcal{J}, \forall r \in \mathcal{R}, \forall y \in \mathcal{Y}, \forall s \in \mathcal{S}, \forall h \in \mathcal{H} \ (\mathbf{54})$$

$$\omega^1_{jrysh-1} - \omega^1_{jrysh} \leq \underline{r_j} \quad ,\forall j \in \mathcal{J}, \forall r \in \mathcal{R}, \forall y \in \mathcal{Y}, \forall s \in \mathcal{S}, \forall h \in \mathcal{H} \ (\mathbf{55})$$

$$\omega^1_{jrysh} \leq C_{jry}\left(\overline{q_j} - \underline{q_j}\right) \quad ,\forall j \in \mathcal{J}, \forall r \in \mathcal{R}, \forall y \in \mathcal{Y}, \forall s \in \mathcal{S}, \forall h \in \mathcal{H} \ (\mathbf{56})$$

$$\omega^1_{jrysh} \leq u_{jrysh}\Omega \quad ,\forall j \in \mathcal{J}, \forall r \in \mathcal{R}, \forall y \in \mathcal{Y}, \forall s \in \mathcal{S}, \forall h \in \mathcal{H} \ (\mathbf{57})$$

$$\omega^2_{jrysh} \leq C_{jry}\underline{q_j} \quad ,\forall j \in \mathcal{J}, \forall r \in \mathcal{R}, \forall y \in \mathcal{Y}, \forall s \in \mathcal{S}, \forall h \in \mathcal{H} \ (\mathbf{58})$$

$$\omega^2_{jrysh} = C_{jry}\underline{q_j} - \left(1 - u_{jrysh}\right)\Omega + s_{jrysh} \quad ,\forall j \in \mathcal{J}, \forall r \in \mathcal{R}, \forall y \in \mathcal{Y}, \forall s \in \mathcal{S}, \forall h \in \mathcal{H} \ (\mathbf{59})$$

$$s_{jrysh} \leq \left(1 - u_{jrysh}\right)\Omega - C_{jry}\underline{q_j} + u_{jrysh}\Omega \quad ,\forall j \in \mathcal{J}, \forall r \in \mathcal{R}, \forall y \in \mathcal{Y}, \forall s \in \mathcal{S}, \forall h \in \mathcal{H} \ (\mathbf{60})$$

$$x_{jrysh} \geq \sum_{h' > h - M^U_j} z_{jrysh} \quad ,\forall j \in \mathcal{J}, \forall r \in \mathcal{R}, \forall y \in \mathcal{Y}, \forall s \in \mathcal{S}, \forall h \in \mathcal{H} \ (\mathbf{61})$$

$$1 - x_{jrysh} \geq \sum_{h' > h - M^D_j} v_{jrysh} \quad ,\forall j \in \mathcal{J}, \forall r \in \mathcal{R}, \forall y \in \mathcal{Y}, \forall s \in \mathcal{S}, \forall h \in \mathcal{H} \ (\mathbf{62})$$

$$B_{jrysh} = B_{jrysh-1} + \sqrt{\eta_j}\Delta^+_{jrysh} - \frac{\Delta^-_{jrysh}}{\sqrt{\eta_j}} \quad ,\forall j \in \mathcal{B}, \forall r \in \mathcal{R}, \forall y \in \mathcal{Y}, \forall s \in \mathcal{S}, \forall h \in \mathcal{H} \ (\mathbf{63}\boldsymbol{a})$$

$$B_{jrysh} = B_{jrysh-1} + \sqrt{\eta_j}\Delta^+_{jrysh} - \frac{\Delta^-_{jrysh}}{\sqrt{\eta_j}} + I_{rysh} \quad ,\forall j \in \mathcal{B}, \forall r \in \mathcal{R}, \forall y \in \mathcal{Y}, \forall s \in \mathcal{S}, \forall h \in \mathcal{H} \ (\mathbf{63}\boldsymbol{b})$$

$$B_{jrysh} = B_{jrysh-1} - \frac{\Delta^-_{jrysh}}{\sqrt{\eta_j}} + I_{rysh} \quad ,\forall j \in \mathcal{B}, \forall r \in \mathcal{R}, \forall y \in \mathcal{Y}, \forall s \in \mathcal{S}, \forall h \in \mathcal{H} \ (\mathbf{63}\boldsymbol{c})$$

$$B_{jrysh} \leq \overline{\mathrm{B}_j}C_{jry} \quad ,\forall j \in \mathcal{B}, \forall r \in \mathcal{R}, \forall y \in \mathcal{Y}, \forall s \in \mathcal{S}, \forall h \in \mathcal{H} \ (\mathbf{64})$$

$$B_{jrysh} \geq \underline{\mathrm{B}_j}C_{jry} \quad ,\forall j \in \mathcal{B}, \forall r \in \mathcal{R}, \forall y \in \mathcal{Y}, \forall s \in \mathcal{S}, \forall h \in \mathcal{H} \ (\mathbf{65})$$

$$\Delta^+_{jrysh} \leq \left(1 - l_{jrysh}\right)\left(\overline{\mathrm{B}_j}C_{jry} - B_{jrysh}\right) \quad ,\forall j \in \mathcal{B}, \forall r \in \mathcal{R}, \forall y \in \mathcal{Y}, \forall s \in \mathcal{S}, \forall h \in \mathcal{H} \ (\mathbf{66})$$

$$\Delta^-_{jrysh} \leq l_{jrysh}\left(B_{jrysh} - \underline{\mathrm{B}_j}C_{jry}\right) \quad ,\forall j \in \mathcal{B}, \forall r \in \mathcal{R}, \forall y \in \mathcal{Y}, \forall s \in \mathcal{S}, \forall h \in \mathcal{H} \ (\mathbf{67})$$

$$B^{EV}_{rysh} = B^{EV}_{rysh-1} + \sqrt{\eta^{EV}_j}{\Delta^{EV}_{rysh}}^+ - \frac{{\Delta^{EV}_{rysh}}^- + k^{EV}\phi_{[h,h+1]}\alpha^{EV}_{ry}NV_{ry}}{\sqrt{\eta^{EV}_j}} \quad ,\forall r \in \mathcal{R}, \forall y \in \mathcal{Y}, \forall s \in \mathcal{S}, \forall h \in \mathcal{H} \ (\mathbf{68})$$

$$B^{EV}_{rysh} \leq \overline{\mathrm{B}^{EV}}\alpha^{EV}_{ry}NV_{ry} \quad ,\forall r \in \mathcal{R}, \forall y \in \mathcal{Y}, \forall s \in \mathcal{S}, \forall h \in \mathcal{H} \ (\mathbf{69})$$

$$B^{EV}_{rysh} \geq \left(\underline{\mathrm{B}^{EV}} + k^{EV}\phi_{[h,h+1]}\right)\alpha^{EV}_{ry}NV_{ry} \quad ,\forall r \in \mathcal{R}, \forall y \in \mathcal{Y}, \forall s \in \mathcal{S}, \forall h \in \mathcal{H} \ (\mathbf{70})$$

$${\Delta^{EV}_{rysh}}^+ \leq \left(1 - l^{EV}_{rysh}\right)\left(\overline{\mathrm{B}^{EV}}\alpha^{EV}_{ry}NV_{ry} - B^{EV}_{rysh}\right) \quad ,\forall r \in \mathcal{R}, \forall y \in \mathcal{Y}, \forall s \in \mathcal{S}, \forall h \in \mathcal{H} \ (\mathbf{71})$$

$$\Delta^{EV}_{rysh}{}^{-} \leq l^{EV}_{rysh}\left(B^{EV}_{rysh} - \left(\underline{\mathrm{B}^{EV}} + k^{EV}\phi_{[h,h+1]}\right)\alpha^{EV}_{ry} NV_{ry}\right) \quad ,\forall r \in \mathcal{R}, \forall y \in \mathcal{Y}, \forall s \in \mathcal{S}, \forall h \in \mathcal{H} \ (\mathbf{72})$$

Note that the optimal level of investment must both satisfy equations **(44)** and **(45)** simultaneously. Therefore, there exist one single set of optimal investment solutions and several distinct set of solutions for the optimal dispatch. We note the vector of solutions for the optimal dispatching problem facing trajectory $\mathfrak{t} \in \mathfrak{T}$ as $\mathfrak{S}^{\mathfrak{t}} = \left(\boldsymbol{q}^{\mathfrak{t}}, \boldsymbol{\omega 1}^{\mathfrak{t}}, \boldsymbol{\omega 2}^{\mathfrak{t}}, \boldsymbol{s}^{\mathfrak{t}}, \boldsymbol{R}^{\mathfrak{t}}, \boldsymbol{\kappa}^{\mathfrak{t}}, \boldsymbol{\chi}^{\mathfrak{t}}, \boldsymbol{\Delta}^{+\mathfrak{t}}, \boldsymbol{\Delta}^{-\mathfrak{t}}, \boldsymbol{B}^{\mathfrak{t}}, \boldsymbol{\Delta}^{+\boldsymbol{EV}^{\mathfrak{t}}}, \boldsymbol{\Delta}^{-\boldsymbol{EV}^{\mathfrak{t}}}, \boldsymbol{B}^{\boldsymbol{EV}^{\mathfrak{t}}}, \boldsymbol{u}^{\mathfrak{t}}, \boldsymbol{z}^{\mathfrak{t}}, \boldsymbol{v}^{\mathfrak{t}}, \boldsymbol{l}^{\mathfrak{t}}, \boldsymbol{l}^{\boldsymbol{EV}^{\mathfrak{t}}}\right)$. For sake of clarity, we drop the superscript $\mathfrak{t}$ for decision variables in the model equations.

The objective function **(43)** can be decomposed as the discounted sum of three components. The first one corresponds to the sum of annuities and fixed operations and maintenance (FOM) costs for cumulated investments in new generation capacities; the second one corresponds to short-term variable and start-up costs, in addition to CO2 costs for thermal technologies. Finally, the third part corresponds to the sum of annuities and FOM for cumulated new investments in transmission capacities. This third component is divided by two as new investments are made for arcs between each pair of regions. The parameter ϑ is a tuning parameter corresponding to the approximate number of weeks for each season. We set it equal to 13.

Equations **(44)** corresponds to the primary frequency control constraint, stating that frequency must remain in an interval D^{lim} around its nominal value. We set it to equal to ∓ 10 mHz. **(45) - (46)** correspond to the flow balance and flow capacity constraints, where q^{+}_{rysh} is the net output power; **(47) - (50)** correspond to the dynamic of generation and transmission installed capacities and new investments.

Equations **(51) - (60)** together formalize constraints on commitment state, start-up and shut-down decisions and maximum and minimum stable power, while keeping our framework linear. We combine the big-M method and the use of slack variables to express minimum production level constraints as a system of linear equations. For Ω big enough, $\omega^{1}_{jrysh} \leq C_{jry}\left(\overline{q_j} - \underline{q_j}\right)$ if u_{jrysh} is equal to 1 and $\omega^{1}_{jrysh} \leq 0$ otherwise. Similarly, $\omega^{2}_{jrysh} = C_{jry}\underline{q_j} + s_{jrysh}$ if u_{jrysh} is equal to 1 and $\omega^{2}_{jrysh} = 0$ otherwise. Indeed, if $u_{jrysh} = 0$, as , ω^{2}_{jrysh} cannot be negative, we have $s_{jrysh} = (1 - u_{jrysh})\Omega - C_{jry}\underline{q_j}$ so that ω^{2}_{jrysh} is null. We see that for $u_{jrysh} = 1$, we necessarily have $s_{jrysh} = 0$ in order to avoid violation of constraint **(60)**, so $\omega^{2}_{jrysh} = C_{jry}\underline{q_j}$. Finally, constraints **(61) – (62)** are used to express minimum up-time and down-time constraints on thermal units.

Equations **(63) – (67)** respectively correspond to the power balance of storage units, state of charge upper and lower limits and upper bounds of electricity inflows and outflows. The use of $\sqrt{\eta_j}$ simply accounts for the fact that a round trip efficiency of η_j is equivalent to an efficiency of storage charge and discharge

of $\sqrt{\eta_j}$. For an arbitrary inflow $a \geq 0$, the amount of electricity stored is equal to $\sqrt{\eta_j}a$, and the amount that is restored to the network is $\sqrt{\eta_j}^2 a = \eta_j a$. As we assume that η_j is constant in time, the process is additive. Equation **(63a)** describes the power balance of batteries, while equations **(63b)** and **(63c)** respectively describe he power balances of reservoirs and hydraulic pumped storage stations. I_{rysh} corresponds to the water inflow coming from precipitations, expressed in MW. Equations **(68) – (72)** translate the same set of constraints for EV, with equation **(70)** ensuring that for each period the state of charge is high enough so EV can drive the average number of kilometers driven in the following period.

Appendix to III.2.1.:

We present a simple method for estimating empirically observed (ie data-driven) level and volatility-maximizing RD components trajectories. In order to respect the correlation of parameters between regions and RD components, we estimated these trajectories at the national level in order to identify in the data the weeks corresponding to the trajectories of interest. We chose $T = 168$ hours and estimate trajectories for each season.

We start by normalizing the values observed for electricity load, noted D_{ysh} for given year y, season s and hour h. Taking reference year y^*, the normalized consumption $\widetilde{D_{ysh}}$ corresponds to the consumption that would have been observed in year y if the demographic, GDP and energy efficiency growth rates observed in the interval $[y, y^*]$ are applied to D_{ysh}. For instance, assume $D_{2017sh} = 50$ GW and take 2018 as reference year. With a GDP growth rate of 2% and a 1% growth rate in energy efficiency gains, then we have $\widetilde{D_{2017sh}} \approx 50{,}49$ GW. The normalization is performed using the following sectorial decomposition formula, for $y < y^*$:

$$\widetilde{D_{ysh}} = \prod_{y<y'\leq y^*} \left[\sum_{f \in \mathcal{F}} \theta_f^h \left(\frac{1+\alpha_{fy'}}{1+\eta_{fy'}} \right) \right] D_{ysh}$$

, where $\mathcal{F}$ is the set of electricity consuming sectors, θ_f^h is the average load share of sector f, $\alpha_{fy'}$ is the GDP growth rate (demographic growth rate for residential sector) of sector f in year y', and $\eta_{fy'}$ is the energy efficiency gains growth rate. We implicitly perform a homothetic transform to each point of demand distribution. The normalized RD can thus be expressed as follows:

$$\widetilde{\mathcal{R}_{ysh}} = \widetilde{D_{ysh}} - \sum_{j \in \mathcal{P}} C_{jy} Z_{2ysh} + \sum_{j \in \mathcal{W}} C_{jy} Z_{3ysh}$$

Z_{2ysh} and Z_{3ysh} correspond to the observed photovoltaic and wind generation units capacity factors. The RD level-maximizing week for each season is thus the vector of hours $\boldsymbol{h_s^L} = (h_{1s}^L, \dots, h_{Ts}^L)$ that maximizes the above expression:

$$\boldsymbol{h_s^L} = \arg\max_h \widetilde{\mathcal{R}_{ysh}}$$

In order to estimate the volatility-maximizing week for each season, we start by scaling each component of RD such that they take values between 0 and 1. As Z_{2ysh} and Z_{3ysh} are not directly observed in the data, we obtain them by dividing the solar and wind power outputs by photovoltaic and wind plants installed capacities respectively. Electricity load is standardized by subtracting for all value $\widetilde{D_{ysh}}$ the minimum value from the distribution of $\widetilde{D_{ysh}}$ and dividing it by the range of the distribution. We note $\widetilde{d_{ysh}}$ the normalized demand. As we are interested in measuring variations of residual demand, this standardization is necessary so the differences in ranges of RD components are neutralized. However, the variability of RD trajectories is both a variable of RES installed capacities and the share of RES capacities in total electricity load. Thus, the selection of the most-volatile RD week in the data must be informed by the share of RES in the electricity mix that is targeted. Formally, we define the simulated RD as follows:

$$\mathcal{R}_{ysh}^{SIMU}(p,x) = px\widetilde{d_{ysh}} - \sum_{j\in\mathcal{P}} xZ_{2ysh} + \sum_{j\in\mathcal{W}} xZ_{3ysh} = x\left(p\widetilde{d_{ysh}} - \sum_{j\in\mathcal{P}} Z_{2ysh} + \sum_{j\in\mathcal{W}} Z_{3ysh}\right)$$

x corresponds to the volume of installed capacity that is targeted for RES. It is chosen equal for solar and wind generation technologies. p can be related to the share of RES in the electricity mix. For $p = 4$ for instance, the amount of installed capacity is approximately equal to 50% of electricity demand. For $p = 6$, it is roughly equal to 33%. For a given value of p, $\mathcal{R}_{ysh}^{SIMU}(p,x)$ is estimated for $x \in [0, \overline{x}]$, where $\overline{x}$ is calibrated using the peak load observed in the data. Noting the peak load D^+, we have $\overline{x} = \left\lfloor \frac{D^+}{p} \right\rfloor$, such that $\overline{x}p\widetilde{d_{ysh}} \approx D^+$. This ensures that the values of x used for estimating $\mathcal{R}_{ysh}^{SIMU}(p,x)$ reflect the true range of electricity demand. Then, the total weekly variation of the simulated RD for given season and year is given by:

$$\mathcal{R}_{ys}^{SIMU,VAR}(p,x) = \int_0^T \left|\dot{\mathcal{R}_{ys\tau}^{SIMU}}(p,x)\right| d\tau$$

Finally, it is possible to express the total weekly variation as a score by dividing it by the maximum weekly variation observed. Using French data from RTE on the electricity consumption, solar and wind power production on the period 2013-2018, we obtain the following graph for all weeks of spring:

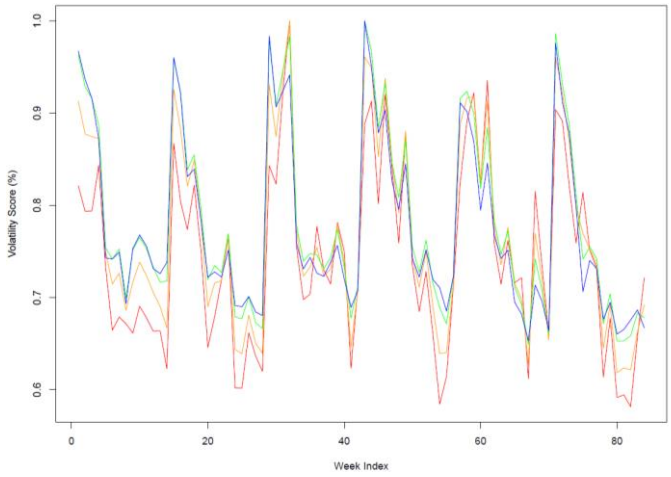

Figure 8: Weekly RD variability score for spring weeks

The red, orange, green and blue lines respectively correspond to RD weekly variability scores with RES installed capacities equal to 100%, 66%, 50% and 40% approximately. The striking feature of **Figure 8** is that while some weeks exhibit very high variability scores for 100% RES, the score drastically increases when the share of RES in the electricity mix increases as well (approx. week 62 for instance). On the contrary, some weekly RD patterns become increasingly problematic, in terms of flexibility requirement from the generation mix, when the RES share of approximately 40%. Thus, based on the RES penetration target, it is possible to select one (or several, with increased computational costs though) weeks based on this variability score.

Appendix to III.2.2:

	> 1 GWe	**> 3 GWe**	**> 5 GWe**
	ET	ET	ET
Combined cycle gas turbine	10.8/9.45	10.35/9.45	11.7/11.25
Gas turbine	1.5/2.7	1.5/2.1	0.9/1.5
Nuclear	10.8/9.6	9.6/9.6	8/8
Wind	0/0	0/0	0/0.03
Utility-scale PV	1/1	3/3.04	5/4.97
Commercial PV	0/0	0/0	0/0
Residential PV	0/0	0/0	0/0
Battery storage	6.32/7.34	12.74/12.9	13.08/13.2

Table 6: Optimal investment level by technology, with constraints on minimum installed capacities for renewables and maximum on CO2 emitting power plants (Empirical trajectories, minimum-maximum-level robust vs. minimum-maximum-level-robust and variability-robust

> 1 GWe	Adapted mix (empirical)	Non-adapted mix (empirical)
Yearly fixed costs & annuities (M€)	4246	4273
Variable costs (level-maximizing week) (M€)	137.1	122.6
Variable costs (level-minimizing week) (M€)	46.65	47.12
Variable costs (variability-maximizing week) (M€)	92.21	INF
> 3 GWe		
Yearly fixed costs & annuities (M€)	4512	4548
Variable costs (level-maximizing week) (M€)	133.9	122.5
Variable costs (level-minimizing week) (M€)	45.64	45.38
Variable costs (variability-maximizing week) (M€)	88.6	INF
> 5 GWe		
Yearly fixed costs & annuities (M€)	4216	4223
Variable costs (level-maximizing week) (M€)	185.34	132.18
Variable costs (level-minimizing week) (M€)	54.69	54.81
Variable costs (variability-maximizing week) (M€)	97.82	INF

Table 7: Cost decomposition of the electricity mix, with constraints on minimum installed capacities for renewables and maximum on CO2 emitting power plants (Empirical trajectories, minimum-maximum-level robust vs. minimum-maximum-level-robust and variability-robust)

Declarations: Not applicable

Bibliography:

ALVAREZ-LOPEZ Juan & KUMARASWAMY Ponnambalam, "Long-term uncertainty evaluation of pool electricity markets", *Energy Policy*, Elsevier, vol.38, n°2, 2010, pp.840-849

BABONNEAU F., VIAL J.-P., APPARIGLIATO R., "Robust Optimization for Environmental and Energy Planning" in *Uncertainty and Environmental Decision Making: A Handbook of Research and Best Practice*, 2009, pp.79-126

BELLMAN R., "Dynamic Programming", Princeton University Press, Princeton, New Jersey, 1957

BEN-TAL A. & NEMIROVSKI A., "Robust solutions of linear programming problems contaminated with uncertain data", *Mathematical Programming*, vol.88, 2000, pp.411-424

BERTSEKAS Dimitri P., *Dynamic Programming and Optimal Control*, Athena Scientific, 1995

BERTSIMAS D. & SIM M., "Price of robustness", *Operations Research*, vol.52, 2004, pp.35-53

BIRGE John R. & LOUVEAUX François, *Introduction to Stochastic Programming*, Springer, 1997

CANY C., MANSILLA C., MATHONNIERE G., DA COSTA P., "Nuclear contribution to the penetration of variable renewable energy sources in a French decarbonized power mix", *Energy*, vol.150, 2018, pp.544-555

CHARNES A. & COOPER W. W., "Chance-Constrained Programming", *Management Science*, vol.6, n°1, 1959, pp.73-79

CHEN Xin, SIM Melvyn, SUN Peng, "A Robust Optimization Perspective on Stochastic Programming", *Operations Research*, vol.55, n°6, 2007, pp.1058-1071

CHEN Yue, WEI Wei, LIU Feng, MEI Shengwei, "Distributionally robust hydro-thermal-wind economic dispatch", *Applied Energy*, vol.173, 2016, pp.511-519

CHEN Zhi, SIM Melvyn, XU Huan, "Distributionally Robust Optimization with Infinitely Constrained Ambiguity Sets", *Operations Research*, vol.67, n°5, 2019

DELAGE Erick & YE Yinyu, "Distributionally Robust Optimization under Moment Uncertainty with Application to Data-Driven Problems", *Operations Research*, vol.58, n°3, 2010

DE SISTERNES Fernando & PARSONS John E., "The Impact of Uncertainty on the Need and Design of Capacity Remuneration Mechanisms in Low-Carbon Power Systems", MIT CEEPR, February 2016

DONG Lei, LI Jia, PU Tianjiao, CHEN Naishi, "Distributionally robust optimization model of active distribution network considering uncertainties of source and load", *Journal of Modern Power Systems and Clean Energy*, vol.7, n°6, 2019, pp.1585-1595

GOH Joel & SIM Melvyn, "Distributionally Robust Optimization and Its Tractable Approximations", *Operations Research*, vol.58, n°4, 2010, pp.902-917

GONZALEZ-SALAZAR Miguel Angel, KIRSTEN Trevor, PRCHLIK Lubos, "Review of the operational flexibility and emissions of gas – and coal-fired power plants in a future with growing renewables", *Renewable and Sustainable Energy Review*, vol.82, 2018, pp.1497-1513

JALILVAND-NEJAD Amir, SHAFAEI Rasoul, SHAHRIARI Hamid, "Robust optimization under correlated polyhedral uncertainty set", *Computers & Industrial Engineering*, vol.92, 2016, pp.82-94

KALL Peter & WALLACE Stein W., *Stochastic Programming*, John Wiley & Sons, Chichester, 1994

LEFFONDRE Karen et alii., "Statistical measures Were Proposed for Identifying Longitudinal Patterns of Change in Quantitative Health Indicators", *Journal of Clinical Epidemiology*, vol.57, n°10, 2004, pp.1049-1062

LORCA Alvaro & SUN Xu Andy, "Adaptive Robust Optimization with Dynamic Uncertainty Sets for Multi-Period Economic Dispatch under Significant Wind", *IEEE Transactions on Power Systems*, vol.30, n°4, 2015, pp.1702-1713

MA Hongyan, JIANG Ruiwei, YAN Zheng, "Distributionally Robust Co-Optimization of Power Dispatch and Do-Not Exceed Limits", *IEEE Transactions on Power Systems*, vol.35, n°2, 2020, pp.887-897

NING Chao & YOU Fengqi, "Data-driven decision making under uncertainty integrating robust optimization with principal component analysis and kernel smoothing methods", *Computers and Chemical Engineering*, vol.112, 2018, pp.190-210

POSTEK Krzysztof, BEN-TAL Aharon, DEN HERTOG Dick, MELENBERG Bertrand, "Robust optimization with ambiguous stochastic constraints under mean and dispersion information", *Operations Research*, vol.66, n°3, 2018, pp.814-833

PREKOPA Andras, "On Probabilistic Constrained Programming", Proceedings of the Princeton Symposium on Mathematical Programming, Princeton University Press, 1970, pp.113-138

RAHIMIAN H. & MEHROTRA S., "Distributionally Robust Optimization: A Review", Mathematics, Computer Science, ArXiv, 2019

ROSS Sheldon, *Stochastic Processes*, John Wiley & Sons, 1983

SHANG Chao & YOU Fengqi, "Distributionally robust optimization for planning and scheduling under uncertainty", *Computers and Chemical Engineering*, vol.110, 2018, pp.53-68

SHAPIRO A. & NEMIROVSKI A., "On complexity of stochastic programming problems", in *Continuous Optimization: Current Trends and Modern Applications*, JEYAJUMAR V. & RUBINOV A., Springer, 2005, pp.111-146.

SOYSTER A.L., "Convex programming with set-inclusive constraints and applications to inexact linear programming", *Operations Research*, vol.21, 1973, pp.1154-1157

SYLVESTRE Marie-Pierre et alii., "Classification of Patterns of Delirium Severity Scores Over Time in an Elderly Population", *International Psychogeriatrics*, vol.18, n°4, 2007, pp.667-680

WIESEMANN W., KUHN D., SIM M., "Distributionally Robust Convex Optimization", *Operations Research*, vol.62, 2014, pp.1358-1376

XU Huan & MANNOR Shie, "Distributionally Robust Markov Decision Processes", *Mathematics of Operations Research*, vol.37, n°2, 2012

YUAN Yuan, LI Zukui, HUANG Biao, "Robust optimization under correlated uncertainty: Formulations and computational study", *Computers and Chemical Engineering*, vol.85, 2016, pp.58-71

Retrouvez toute la collection
https://www.ifpenergiesnouvelles.fr/article/les-cahiers-leconomie

IFP SCHOOL
228 - 232 avenue Napoléon Bonaparte
92852 Rueil-Malmaison
www.ifpschool.com

IFP Energies nouvelles
1-4 avenue de Bois-Préau
92852 Rueil-Malmaison
www.ifpenergiesnouvelles.fr